Table 5: Differences in detection rate, according to potency category

Potency category	No. of chemicals	No. of chemicals correctly corresponding to LLNA result	No. of chemicals incorrectly corresponding to LLNA result	Detection rate (%)
Extreme	8	8	0	100.0
Strong	16	14	2	87.5
Moderate	24	22	2	91.7
Weak	23	18	5	78.3
Non-sensitiser	29	22	7	75.9

Detection rate = positive predictivity for sensitisers and negative predictivity for weak/non-sensitisers (grey shading).

rates of weak sensitisers and non-sensitisers (i.e. the ratio of the test chemicals which were correctly evaluated) were 78.3% (sensitivity) and 75.9% (specificity), respectively, both of which are comparatively low. Therefore, it might be difficult for the h-CLAT to distinguish weak sensitisers from non-sensitisers.

Discussion

We compiled a database of h-CLAT results for 100 chemicals, for comparison with existing LLNA data. It is important to select chemicals that display a wide range of sensitising potencies and physicochemical properties, and our set of test chemicals appropriately reflected both the chemical and biological diversity of known sensitisers. It is well known that skin sensitisers must have a relatively low MW (< 500Da) and appropriate physicochemical properties (18, 19). Most of the selected chemicals met these requirements. Furthermore, the distributions of both characteristics were very similar to those of the most extensive LLNA database. Therefore, our database did not show any marked bias.

Our results demonstrate the good predictive performance of the h-CLAT. The accuracy of the h-CLAT *versus* the LLNA was 84%, which can be considered acceptable for a single *in vitro* alternative test. It is especially noteworthy that all eight sensitisers categorised as extreme were correctly judged as positives in the h-CLAT, because the correct prediction of extreme sensitisers is most important for safety assessment. It was reported that the accuracy of the peptide reactivity test *versus* the LLNA was 89%, which is similar to that of the h-CLAT (17). The integration of this cell-based assay and the peptide reactivity assay might improve accuracy when used as an alternative test system, because the two tests have different domains of applicability and different endpoints. The h-CLAT database presented here should be useful, not only in performance evaluation of the h-CLAT as a single examination method, but also for considering possible combination systems with other endpoints.

Basically, most sensitisers showed a dose-dependent increase in CD86 and/or CD54 expression at sub-toxic concentrations. The most frequent pattern was an augmentation of both CD86 and CD54 levels, but there were also many cases in which either CD86 level or CD54 level increased. It is well known that CD86 and CD54 have roles as co-stimulatory molecules and are regulated independently (2). That was the reason why we adopted a battery system consisting of both endpoints, and analysis of the database confirmed the value of this approach. It has been suggested that activation mechanisms vary from sensitiser to sensitiser (20). Python *et al.* (21) concluded that a combination of at least two markers was needed to establish a reliable evaluation of dendritic cell-like activation. Nevertheless, sensitisers that augment either CD86 (e.g. oxazolone) or CD54 (e.g. 1-benzoylacetone) expression, should be useful tools to analyse the signalling pathways of THP-1 cells.

We have evaluated the effect of treatment time, and selected 24 hours as an appropriate treatment period (7, 8). Python *et al.* also found that some sensitisers have time-dependent and chemical-dependent effects on CD86 expression in the U-937 cell line (21). Therefore, it remains possible that both endpoints might be augmented in another cell line, in cases where only one endpoint was enhanced under the conditions used in the present assay (24-hour treatment and sub-toxic doses). However, it is unrealistic to set too many conditions for measurement. We think the current method would be adequate to evaluate a majority of test chemicals, based on our detailed studies on test conditions (8, 16).

There were both false-negative and false-positive results in the h-CLAT, so it is necessary to

clarify the limitations of the assay. A consideration of the false negatives is especially important for clarifying the range of applicability of the h-CLAT. In this assay system, THP-1 cells are directly exposed to chemicals in the culture medium, which is a highly simplified system compared to the skin sensitisation process. The use of such submerged culture systems may involve various limitations, such as lack of solubility of a test chemical in the medium, lack of metabolic activity, and lack of interaction with keratinocytes. Water solubility is a key limiting factor for such a test, and the h-CLAT may be unsuitable for evaluating the sensitising potentials of insoluble compounds. As shown in Table 1, hexyl cinnamic aldehyde, abietic acid and benzoyl peroxide, all of which were false negatives, did not have good solubility in the medium. In our study, eight of nine false negatives were water-insoluble chemicals. It seems that, in the current protocol for the h-CLAT, poor solubility in the medium is the most important limitation. For phthalic anhydride, no cytotoxicity was observed, even at the highest concentration, and cytotoxicity was most-likely limited by the solubility of this compound in DMSO. The use of a vehicle other than DMSO might overcome this limitation.

The expression of cytochrome P450 is up-regulated only when human monocytes differentiate into macrophages (22). This suggests that the metabolic activity of normal monocytic THP-1 cells is not high. Isoeugenol is known to be a prohapten, which requires metabolic activation for allergy induction (23). This may also be the case for benzoyl peroxide (24), and air-oxidation is involved in the development of sensitising potential of abietic acid (25). These sensitisers might have been characterised as false negatives in the h-CLAT, because of the insufficient metabolic activity of THP-1 cells. Therefore, the h-CLAT might not be able to evaluate the sensitising potential of chemicals that are subject to activation by metabolism or air-oxidation.

The responsiveness of THP-1 cells tends to be less than that of DCs (5, 6). Compared with the LLNA, there were five false negatives among 23 weak sensitisers. In addition, the detection rate of weak sensitisers was clearly lower than that of sensitisers categorised as moderate or above.

Some weak sensitisers, such as 1-bromohexane, cyclamen aldehyde and butyl glycidyl ether, might not have been identified, due to the insufficient sensitivity of the test. However, the distinction between weak sensitiser and non-sensitiser in the LLNA is based on an arbitrary threshold, so some discrepancy in the case of weak sensitisers is not surprising.

The fluorescence intensity of FITC-labelled anti-CD86 or CD54 antibody is measured by flow cytometry, as an indicator of the presence of these proteins on the cell surface. Thus, if a chemical that exhibits fluorescence *per se* binds to the cell surface non-specifically, the results may be affected. In other words, intrinsic chemical fluorescence may interfere with the fluorescence of the antibody. Abietic acid, which exhibits fluorescence, induced a significant augmentation of CD54 at the gene expression level (as determined by real-time quantitative RT-PCR), but not at the protein level (as measured by flow cytometry) (unpublished data). Therefore, the fact that it was false negative might be due to its intrinsic fluorescence.

Interestingly, both the bromo-alkanes which were tested in this study were misclassified (1-bromohexane was a false negative and 1-bromobutane was a false positive). Further studies should be carried out, not only to clarify the reason for this contradiction, but also to discuss this issue from the viewpoint of structure–activity relationships.

Because the h-CLAT is a relatively simple model, it could be a useful tool for investigating the mechanisms of skin sensitisation (e.g. the influence of metabolic activity), in addition to providing an alternative method for predicting skin sensitisation effects. Finally, the understanding of various chemical reaction mechanistic domains which are associated with sensitisation should be emphasised, because this understanding is necessary to develop an alternative system for the assay of skin sensitisation (26). Therefore, this comparative evaluation of the h-CLAT *versus* the LLNA should be examined from the viewpoint of this understanding in the future.

Conclusions

We have evaluated 100 test chemicals with a single h-CLAT protocol, and compared the results obtained with the LLNA data. There was a high degree of consistency between the two methods: the accuracy of the h-CLAT was 84% with respect to the LLNA. Possible limitations of the h-CLAT include poor test compound solubility, metabolic activation, and sensitivity.

Received 12.11.09; received in final form 03.05.10; accepted for publication 12.05.10.

References

1. De Silva, O., Basketter, D.A., Barratt, M.D., Corsini, E., Cronin, M.T.D., Das, P.K., Degwert, J., Enk, A., Garrigue, J-L., Hauser, C., Kimber, I., Lepoittevin, J-P., Peguet, J. & Ponec, M. (1996). Alternative methods for skin sensitisation testing. *ATLA* **24**, 683–705.
2. Aiba, S., Terunuma, A., Manome, H. & Tagami, H. (1997). Dendritic cells differently respond to haptens and irritants by their production of cytokines

and expression of co-stimulatory molecules. *European Journal of Immunology* **27**, 3031–3038.
3. Hopper, U., Degwert, J. & Steckel, F. (1995). Use of CD1a$^-$ dendritic cells and keratinocytes to characterize cellular reaction involved in allergic contact dermatitis. *Journal of Cellular Biochemistry* **59**, Suppl. S21A, 11–18.
4. Rougier, N., Redziniak, G., Mougin, D., Schmitt, D. & Vincent, C. (2000). *In vitro* evaluation of the sensitization potential of weak contact allergens using Langerhans-like dendritic cells and autologous T cells. *Toxicology* **145**, 73–82.
5. Ashikaga, T., Hoya, M., Itagaki, H., Katumura, Y. & Aiba, S. (2002). Evaluation of CD86 expression in THP-1 human monocyte cells as predictive endpoints for contact sensitizers. *Toxicology in Vitro* **16**, 711–716.
6. Yoshida, Y., Sakaguchi, H., Ito, Y., Okuda, M. & Suzuki, H. (2003). Evaluation of the skin sensitization potential of chemicals using expression of costimulatory molecules. *Toxicology in Vitro* **17**, 221–218.
7. Ashikaga, T., Yoshida, Y., Hirota, M., Yoneyama, K., Itagaki, H., Sakaguchi, H., Miyazawa, Y., Ito, Y., Suzuki, H. & Toyoda, H. (2006). Development of an *in vitro* skin sensitization test using human cell lines: Human Cell Line Activation Test (h-CLAT). I. Optimization of the h-CLAT protocol. *Toxicology in Vitro* **20**, 767–773.
8. Sakaguchi, H., Ashikaga, T., Miyazawa, Y., Yoshida, Y., Ito, Y., Yoneyama, K., Hirota, M., Itagaki, H., Toyoda, H. & Suzuki, H. (2006). Development of an *in vitro* skin sensitization test using human cell lines: Human Cell Line Activation Test (h-CLAT). II. An inter-laboratory study of the h-CLAT. *Toxicology in Vitro* **20**, 774–784.
9. Sakaguchi, H., Miyazawa, M., Yoshida, Y., Ito, Y. & Suzuki, H. (2007). Prediction of preservative sensitization potential using surface marker CD86 and/or CD54 expression on human cell line, THP-1. *Archives of Dermatological Research* **298**, 427–437.
10. Bocchietto, E., Paolucci, C., Breda, D., Sabbioni, E. & Burastero, S.E. (2007). Human monocytoid THP-1 cell line *versus* monocyte-derived human immature dendritic cells as *in vitro* models for predicting the sensitising potential of chemicals. *International Journal of Immunopathology & Pharmacology* **20**, 259–265.
11. Ashikaga, T., Sakaguchi, H., Okamoto, K., Mizuno, M., Sato, J., Yamada, T., Yoshida, M., Ota, N., Hasegawa, S., Kodama, T., Okamoto, Y., Kuwahara, H., Kosaka, N., Sono, S. & Ohno, Y. (2008). Assessment of the human Cell Line Activation Test (h-CLAT) for skin sensitization: Results of the first Japanese inter-laboratory study. *AATEX* **13**, 27–35.
12. Becker, D., Kuhn, U., Lempertz, U., Enk, A., Saloga, J. & Knop, J. (1997). Flow-cytometric screening for the modulation of receptor-mediated endocytosis in human dendritic cells: Implications for the development of an *in vitro* technique for predictive testing of contact sensitizers. *Journal of Immunological Methods* **203**, 171–180.
13. Gerberick, G.F., Ryan, C.A., Kern, P.S., Schlatter, H., Dearman, R.J., Kimber, I. & Patlewicz, G.Y. (2005). Compilation of historical local lymph node data for evaluation of skin sensitization alternative methods. *Cell Biology & Toxicology* **97**, 417–427.
14. Casati, S., Aeby, P., Kimber, I., Maxwell, G., Ovigne, J-M., Roggen, E., Rovida, C., Tosti, L. & Basketter, D. (2009). Selection of chemicals for development and evaluation of *in vitro* methods for skin sensitisation testing. *ATLA* **37**, 305–312.
15. Potts, R.O. & Guy, R.H. (1992). Predicting skin permeability. *Pharmacological Research* **9**, 663–669.
16. Sakaguchi, H., Ashikaga, T., Masaaki, M., Kosaka, N., Ito, Y., Yoneyama, K., Sono, S., Itagaki, H., Toyoda, H. & Suzuki, H. (2009). The relationship between CD86/CD54 expression and THP-1 cell viability in an *in vitro* skin sensitization test — human Cell Line Activation Test (h-CLAT). *Cell Biology & Toxicology* **25**, 109–126.
17. Gerberick, G.F., Vassallo, J.D., Foertsch, L.M., Price, B.B., Chaney, J.G. & Lepoittevin, J.P. (2006). Quantification of chemical peptide reactivity for screening contact allergens: A classification tree model approach. *Toxicological Sciences* **97**, 417–427.
18. Boss, J.D. & Meinard, M.M. (2000). The 500 Dalton rule for skin penetration of chemical compounds and drugs. *Experimental Dermatology* **9**, 165–169.
19. Smith, C.K. & Hotchkiss, S.A. (2001). Appendix I: *In vivo* sensitisation data and physico-chemical properties of xenobiotics. In *Allergic Contact Dermatitis: Chemical and Metabolic Mechanisms*, pp. 229–236. London, UK: Taylor & Francis.
20. Miyazawa, M., Ito, Y., Kosaka, N., Sakaguchi, H. & Suzuki, H. (2008). Role of MAPK signaling pathway in the activation of dendritic type cell line, THP-1, induced by DNCB and $NiSO_4$. *The Journal of Toxicological Sciences* **33**, 51–59.
21. Python, F., Goebel, C. & Aeby, O. (2007). Assessment of the U-937 cell line for the detection of contact allergens. *Toxicology & Applied Pharmacology* **220**, 112–124.
22. Nakayama, K., Nitto, T., Inoue, T. & Node, K. (2008). Expression of the cytochrome P-450 epoxygenase CYP2J2 in human monocytic leukocytes. *Life Sciences* **29**, 339–345.
23. Smith, C.K. & Hotchkiss, S.A. (2001). Xenobiotics as skin sensitizers: Metabolic activation and detoxication, and protein-binding mechanisms. In *Allergic Contact Dermatitis: Chemical and Metabolic Mechanisms*, pp. 119–205. London, UK: Taylor & Francis.
24. Nacht, S., Yeung, D., Beasley, J.N., Jr, Anjo, M.D. & Maibach, H.I. (1981). Benzoyl peroxide: Percutaneous penetration and metabolic disposition. *Journal of the American Academy of Dermatology* **4**, 31–37.
25. Basketter, D.A., Bremmer, J.N., Buckley, P., Kammuller, M.E., Kawabata, T., Kimber, I., Loveless, S.E., Magda, S., Stringer, D.A. & Vohr, H.W. (1995). Pathology considerations for, and subsequent risk assessment of, chemicals identified as immunosuppressive in routine toxicology. *Food & Chemical Toxicology* **33**, 1051–1056.
26. Roberts, D.W., Patlewicz, G., Kern, P.S., Gerberick, F., Kimber, I., Dearman, R.J., Ryan, C.A., Basketter, D.A. & Aptula, A.O. (2007). Mechanistic applicability domain classification of a local lymph node assay dataset for skin sensitization. *Chemical Research Toxicology* **20**, 1019–1030.

Oxidation of Cell Surface Thiol Groups by Contact Sensitizers Triggers the Maturation of Dendritic Cells

Saori Kagatani[1], Yoshinori Sasaki[1], Morihiko Hirota[2], Masato Mizuashi[1], Mie Suzuki[2], Tomoyuki Ohtani[1], Hiroshi Itagaki[2] and Setsuya Aiba[1]

p38 mitogen-activated protein kinase (MAPK) has a crucial role in the maturation of dendritic cells (DCs) by sensitizers. Recently, it has been reported that the oxidation of cell surface thiols by an exogenous impermeant thiol oxidizer can phosphorylate p38 MAPK. In this study, we examined whether sensitizers oxidize cell surface thiols of monocyte-derived DCs (MoDCs). When cell surface thiols were quantified by flow cytometry using Alexa fluor maleimide, all the sensitizers that we examined decreased cell surface thiols on MoDCs. To examine the effects of decreased cell surface thiols by sensitizers on DC maturation, we analyzed the effects of an impermeant thiol oxidizer, *o*-phenanthroline copper complex (CuPhen). The treatment of MoDCs with CuPhen decreased cell surface thiols, phosphorylated p38 MAPK, and induced MoDC maturation, that is, the augmentation of CD83, CD86, HLA-DR, and IL-8 mRNA, as well as the downregulation of aquaporin-3 mRNA. The augmentation of CD86 was significantly suppressed when MoDCs were pretreated with *N*-acetyl-L-cystein or treated with SB203580. Finally, we showed that epicutaneous application of 2,4-dinitrochlorobenzene on mouse skin significantly decreased cell surface thiols of Langerhans cells *in vivo*. These data suggest that the oxidation of cell surface thiols has some role in triggering DC maturation by sensitizers.

Journal of Investigative Dermatology advance online publication, 30 July 2009; doi:10.1038/jid.2009.229

INTRODUCTION

We have reported that murine Langerhans cells (LCs) upregulate their expression of class II major histocompatibility complex antigen and several co-stimulatory molecules, and consequently augment their antigen-presenting function after painting the skin with sensitizers, whereas chemicals that simply irritate the skin cannot induce this phenomenon (Aiba and Katz, 1990; Ozawa *et al.*, 1996). Consistent with these *in vivo* studies, using human monocyte-derived dendritic cells (MoDCs) or dendritic cells (DCs) derived from $CD34^+$ hematopoietic progenitor cells, we (Aiba *et al.*, 1997, 2000) and others (Coutant *et al.*, 1999; Tuschl *et al.*, 2000; Arrighi *et al.*, 2001; De Smedt *et al.*, 2001; Boisleve *et al.*, 2004; Staquet *et al.*, 2004) have shown *in vitro* that purified DCs respond to a variety of sensitizers, but not to irritants, such as benzalkonium chloride or sodium dodecyl sulfate (SDS), by significantly augmenting their expression of CD54, CD86, HLA-DR, and CCR7, and by increasing their production of proinflammatory cytokines. All these data show that sensitizers can induce the maturation of human DCs independent of the skin environment, suggesting that DCs play a crucial role in sensing simple chemicals that potentially sensitize naive T cells and induce allergic contact sensitivity.

In spite of these observations, however, it still remains undetermined how sensitizers with different chemical structures can activate DCs. Recently, using MoDCs, Arrighi *et al.* (2001), Brand *et al.* (2002), and we (Aiba *et al.*, 2003) have reported that several sensitizers,that is, 2,4-dinitrofluorobenzene (DNFB), 2,4-dinitrochlorobenzene (DNCB), and NiSO4, induce the phosphorylation of p38 mitogen-activated protein kinase (MAPK) and/or extracellular signal-regulated kinases (ERK), and that the phenotypic and functional changes induced by these sensitizers are suppressed by inhibitors of p38 MAPK or ERK. In addition, we have reported that $NiCl_2$ can activate NF-κB in MoDCs.

As for the mechanism by which p38 MAPK is activated by sensitizers in spite of the lack of proven specific receptors, we have reported the role of the redox imbalance in the maturation of DCs induced by sensitizers (Mizuashi *et al.*, 2005); that is, we have shown that all the sensitizers decreased the intracellular reduced/oxidized glutathione ratio (GSH/GSSG ratio) in MoDCs, and that this was accompanied by the phosphorylation of p38 MAPK. Moreover, treatment with *N*-acetyl-L-cystein (NAC), which suppressed the reduction of the GSH/GSSG ratio in MoDCs,

[1]*Department of Dermatology, Tohoku University Graduate School of Medicine, Aoba-ku, Sendai, Japan and* [2]*Shiseido Research Center, Shiseido, Kanazawa-ku, Yokohama, Japan*

Correspondence: Dr Setsuya Aiba, Department of Dermatology, Tohoku University Graduate School of Medicine, 1-1 Seiryo-machi, Aoba-ku, Sendai 980-8574, Japan. E-mail: aiba@mail.tains.tohoku.ac.jp

Abbreviations: Ab, antibody; AQP3, aquaporin-3; CuPhen, o-phenanthroline copper complex; DC, dendritic cell; DNCB, 2,4-dinitrochlorobenzene ERK, extracellular signal-regulated kinases; GSH, reduced glutathione GSSG, oxidized glutathione; JNK, c-Jun N-terminal kinase; LC, Langerhans cell; MAPK, mitogen-activated protein kinase; MoDC, monocyte-derived dendritic cell; NAC, N-acetyl-L-cystein; SAPK, stress-activated protein kinase

Received 14 August 2008; revised 1 June 2009; accepted 19 June 2009

abrogated both the phosphorylation of p38 MAPK and the augmentation of CD86 expression by MoDCs.

Recently, it has been reported that oxidation of cell surface thiols in human monocyte cell line, U937, decreases the intracellular GSH content and phosphorylates p38 MAPK (Filomeni *et al.*, 2003). In addition, we have also shown that the oxidation of cell surface thiols can stimulate human monocyte cell line, THP-1, to show the phenotypic changes that characterize the maturation of DCs, for example, the augmentation of CD86 expression and MIP-1β production, and that these phenotypic changes are mainly mediated by the activation of p38 MAPK (Hirota *et al.*, 2009). Moreover, by examining the effects on cell surface thiols of THP-1 by 35 skin sensitizers and 17 non-sensitizers, we have found that most sensitizers significantly reduce cell surface thiols, whereas non-sensitizers except for Tween80 and resorcinol do not (Suzuki *et al.*, 2009). Therefore, we hypothesized that sensitizers oxidize the cell surface thiols of MoDCs, leading to the phosphorylation of p38 MAPK and their maturation. Therefore, in this study, we showed whether sensitizers decrease the cell surface thiols. Next, we showed that an impermeant thiol oxidizer, *o*-phenanthroline copper complex (CuPhen), decreases the cell surface thiols of MoDCs and phosphorylates p38 MAPK, and induces MoDC maturation. Finally, we examined whether epidermal LCs also decrease the cell surface thiols after hapten application on the skin.

RESULTS

All contact sensitizers, but not non-sensitizers, at sublethal concentrations, decreased cell surface thiols of MoDCs and increased their phosphorylated p38 MAPK

As we have reported that some of the sensitizers decreased the intracellular GSH/GSSG ratio in MoDCs, phosphorylated p38 MAPK, and augmented their CD86 expression, in this study, we examined whether sensitizers decrease the cell surface thiols on MoDCs by flow cytometry using an Alexa fluor C_5 maleimide (Invitrogen, Carlsbad, CA), a specific impermeant thiol-reactive compound able to covalently bind to membrane surface cysteines (Figure 1). When we treated MoDCs with various sensitizers, a non-sensitizer, SDS, and a representative danger signal, ATP, for 2 hours, all the sensitizers decreased the exofacial thiol groups in a dose-dependent manner, whereas SDS or ATP did not significantly alter them. In addition, only the sensitizers phosphorylated p38 MAPK of MoDCs. Again, SDS or ATP did not significantly increase phosphorylated p38 MAPK. When we examined the cell viability 2 hours after chemical treatment, it was more than 80% in the concentration used in this experiment. To further clarify the relationship between cell surface thiol expression and phosphorylation of p38 MAPK, we examined the correlation between the relative fluorescence intensity of cell surface thiols stained by Alexa fluor C_5 maleimide and the relative fluorescence intensity of phospho-p38 MAPK stained by anti-phospho-p38 MAPK antibody (Ab) in MoDCs treated with various concentrations of chemicals. The results showed a significant inverse correlation between them.

An impermeant thiol oxidizer, CuPhen, decreased cell surface thiols of MoDCs, phosphorylated p38 MAPK, and activated MoDCs

Ciriolo *et al.* (1993) and Filomeni *et al.* (2003) reported that reducing/oxidizing impermeant agents could affect the intracellular redox state by translocation of their equivalents from the external to the intracellular space. As our current studies revealed that sensitizers decreased the cell surface thiols, we next examined whether the oxidation of cell surface thiols affected the phosphorylation of p38 MAPK of MoDCs and activated them. In this study, we used CuPhen as an impermeant thiol oxidizer (Duncan and Lawrence, 1989; Lawrence *et al.*, 1996). When MoDCs were treated with three different concentrations of CuPhen, that is, 1, 2, and 3 μM, for different time periods, those treated with 2 and 3 μM of CuPhen decreased their cell surface thiol group from 15 minutes after treatment, reaching to a statistically significant level at 2 hours after treatment (Figure 2a and b). Moreover, 2 and 3 μM of CuPhen phosphorylated p38 MAPK 1 hour after treatment, whereas 3 μM of CuPhen phosphorylated it 2 hours after treatment (Figure 2c). It was also confirmed by flow cytometry; that is, when we examined phosphorylated p38 MAPK of MoDCs 2 hours after CuPhen treatment by flow cytometry, 3 μM of CuPhen induced a right shift of the single peak of phosphorylated p38 MAPK in four independent experiments. In addition, both the concentrations of CuPhen also phosphorylated p42/44 ERKs (Figure 2d), although neither concentrations of CuPhen significantly affected phosphorylation of stress-activated protein kinase/c-Jun *N*-terminal kinase (SAPK/JNK) (Figure 2e) or IκB (Figure 2f). When we examined the cell viability 2 hours after chemical treatment, it was more than 80% in the concentration used in this experiment. After 24 hours culture, 2 and 3 μM of CuPhen significantly augmented HLA-DR, CD86, and CD83 expression, although 3 μM of CuPhen significantly decreased the cell viability (Figure 3a). As for maturation markers of MoDCs, other than these phenotypic changes, we also examined IL-8 and aquaporin-3 (AQP3) mRNA expression by MoDCs treated with CuPhen, as de Baey and Lanzavecchia (2000) reported that AQP3 mRNA expression is downregulated during DC maturation. Consistent with the augmentation of CD86 expression, 2 and 3 μM of CuPhen significantly augmented IL-8 mRNA and suppressed AQP3 mRNA expression by MoDCs (Figure 3b).

NAC blocked the reduction of the cell surface thiols of MoDCs induced by CuPhen and suppressed DC maturation

Next, we pretreated MoDCs with NAC 30 minutes before the treatment with CuPhen. NAC is a well-known thiol antioxidant, and suppresses JNK, p38 MAPK, redox-sensitive activating protein-1, and NF-κB transcription factor activities (reviewed by Zafarullah *et al.* (2003)). The treatment of MoDCs with NAC significantly increased the cell surface thiols and suppressed their reduction induced by the treatment with CuPhen (Figure 4a). Consistent with the effects on the cell surface thiols, NAC suppressed the phosphorylation of p38 MAPK (Figure 4b and c) and MoDC maturation

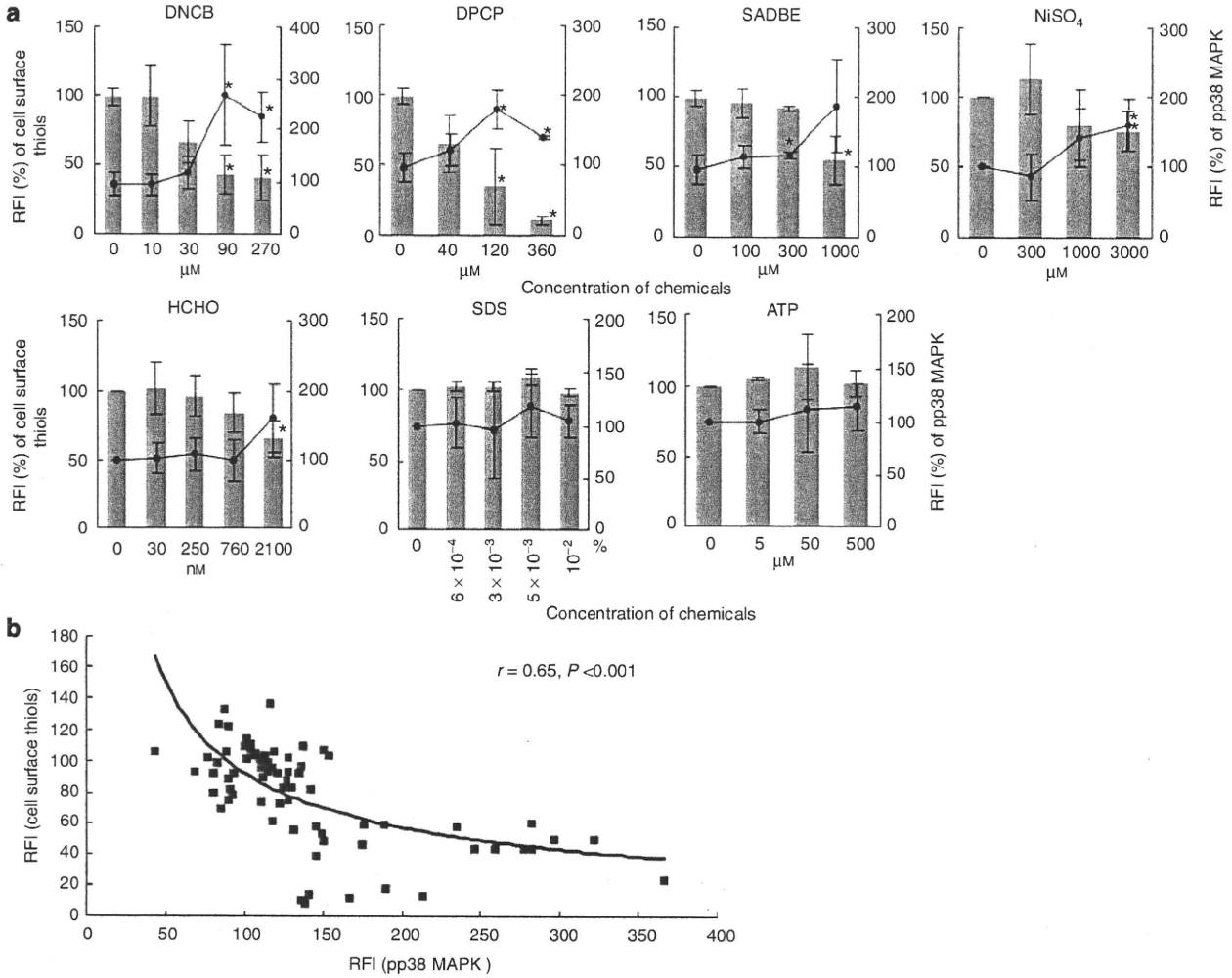

Figure 1. Sensitizers decrease cell surface thiols and phosphorylate p38 MAPK. MoDCs were treated with various concentrations of contact sensitizers, SDS, or ATP for 2 hours. The cell surface thiols were quantified by flow cytometry using thiol-reactive Alex Fluor 488 C5 maleimide. In addition, the intracellular expression of phospho-p38 MAPK (pp38 MAPK) was analyzed by flow cytometry using PE-conjugated anti-pp38 MAPK. (**a**) The mean ± SEM of RFI for cell surface thiols and pp38 MAPK from three to five independent experiments is shown. Asterisks indicate significance (*$P<0.05$) for the difference between stimulated cells and the vehicle-treated control. (**b**) RFIs for cell surface thiols and pp38 MAPK from three to five independent experiments are plotted and analyzed by Pearson's correlation coefficient. RFI, relative fluorescence intensity.

induced by CuPhen (Figure 4d). Interestingly, NAC also rescued the reduction of the cell viability by the treatment with 2 μM CuPhen.

SB203580 suppressed the DC maturation induced by CuPhen

Next, we treated MoDCs with SB203580 to confirm that the stimulation with CuPhen is really mediated through p38 MAPK. The treatment of MoDCs with SB203580 significantly suppressed the augmentation of CD86 expression by CuPhen (Figure 5).

Murine epidermal LCs also decreased the cell surface thiols after DNCB painting

These *in vitro* studies suggest that the reduction of the cell surface thiols of DCs treated with sensitizers induced the signal for DC maturation. We next examined whether epicutaneous application of a representative hapten, DNCB, induced the reduction of the cell surface thiols of epidermal LC. At 2 hours after DNCB painting, epidermal LC that were identified as epidermal $CD86^+$ cells decreased the cell surface thiols (Figure 6).

DISCUSSION

Recently, Tanaka *et al.* (2005) have reported that cell surface thiols other than glutathione regulate signal transduction, leading to phosphorylation of protein kinase B and activation of endothelial nitric oxide synthase. On the other hand, Filomeni *et al.* (2003) have suggested that the oxidation of cell surface thiols by exogenous impermeant GSSG can phosphorylate p38 MAPK. As it has been shown by several researchers that sensitizers phosphorylate p38 MAPK and that the DC maturation induced by sensitizers is at least partly mediated by activated p38 MAPK (Arrighi *et al.*, 2001; Brand *et al.*, 2002; Aiba *et al.*, 2003), in this study, we examined

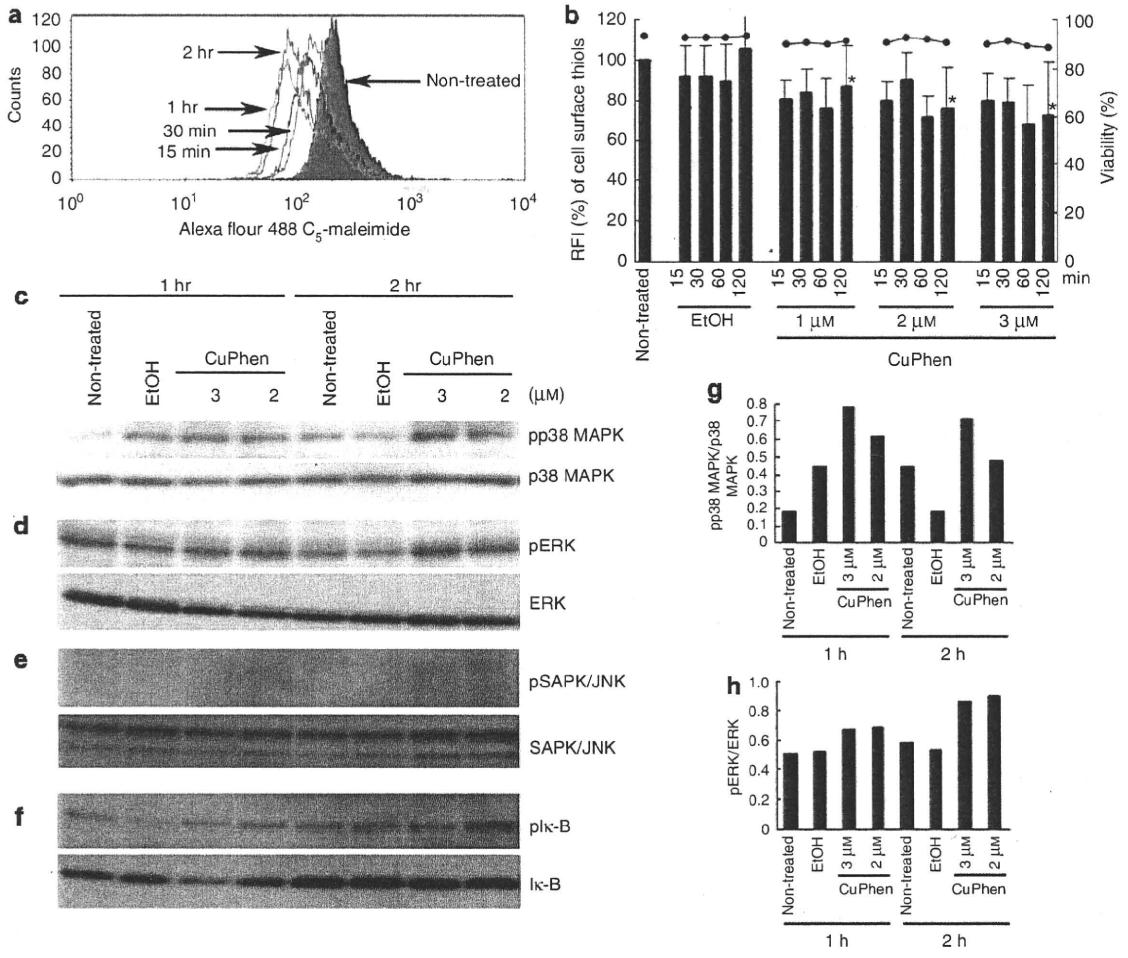

Figure 2. An impermeant thiol oxidizer, CuPhen, decreases cell surface thiols of MoDCs and phosphorylates p38 MAPK. MoDCs were treated with three different concentrations of CuPhen for different time periods. The cell surface thiols were quantified by flow cytometry using thiol-reactive Alex Fluor 488 C5 maleimide. A representative flow cytometry of MoDC treated with 3 μM CuPhen (**a**) and the summarized data from five different experiments (**b**) are presented. The mean ± SEM of RFI is shown by black bars. A line chart shows cell viability. Asterisks indicate significance ($*P<0.05$) for the difference between stimulated cells and the vehicle-treated control. After 1 or 2 hours of treatment with CuPhen, phosphorylation of p38 MAPK was examined by western blotting using anti-pp38 MAPK antibody (**c**), anti-phospho-p42/44 ERKs antibody (**d**), phospho-SAPK/JNK antibody (**e**), or anti-serine (Ser32/36) phosphorylated IκB antibody (**f**). As a control to confirm that equal amounts of protein were loaded to the gel, p38 MAPK, p42/44 ERKs, SAPK/JNK, and IκB expression are also shown. To show the relative ratio of phosphorylated p38 MAPK *versus* total p38 MAPK (**g**) or phosphorylated p42/44 ERKs *versus* total p42/44 ERKs (**h**), the optical densities of the signals were measured with NIH image. These are representative data from two to four different experiments. RFI, relative fluorescence intensity.

whether sensitizers decreased cell surface thiols. The sensitizers that we examined, that is, DNCB, NiSO4, formalin, dephencyprone, and squaric acid dibutyl ester, significantly decreased the cell surface thiols of MoDCs, whereas a representative irritant, SDS, or a danger signal, ATP, did not affect them at all.

Given that sensitizers can penetrate into the cytoplasm and affect the intracellular redox balance, it is not clear whether the oxidation of cell surface thiols of MoDCs by sensitizers induces p38 MAPK and DC maturation. Therefore, we next examined whether an impermeant thiol oxidizer, CuPhen (Duncan and Lawrence, 1989; Lawrence *et al.*, 1996), can phosphorylate p38 MAPK of MoDCs and stimulate DC maturation. After we confirmed that CuPhen decreased cell surface thiols of MoDCs, we showed that CuPhen phosphorylated p38 MAPK and induced DC maturation, that is, the augmentation of HLA-DR, CD83, and CD86 expression, the induction of IL-8 mRNA, and the downregulation of AQP3 mRNA. These data suggest that the oxidation of cell surface thiols by sensitizers can trigger the maturation of MoDCs.

In our previous paper, we reported that NAC recovered the decreased intracellular GSH/GSSG ratio induced by sensitizers and, concomitantly, abrogated the phosphorylation of p38 MAPK and the augmentation of CD86 expression by MoDCs. Recently, it was reported that some effects of NAC, for example, inhibition of apoptosis, antiproliferative effect, inhibition of epidermal growth factor receptor activation, or enhancement of IL-1-induced inducible nitric oxide synthase expression, seemed not to be mediated by an increase of

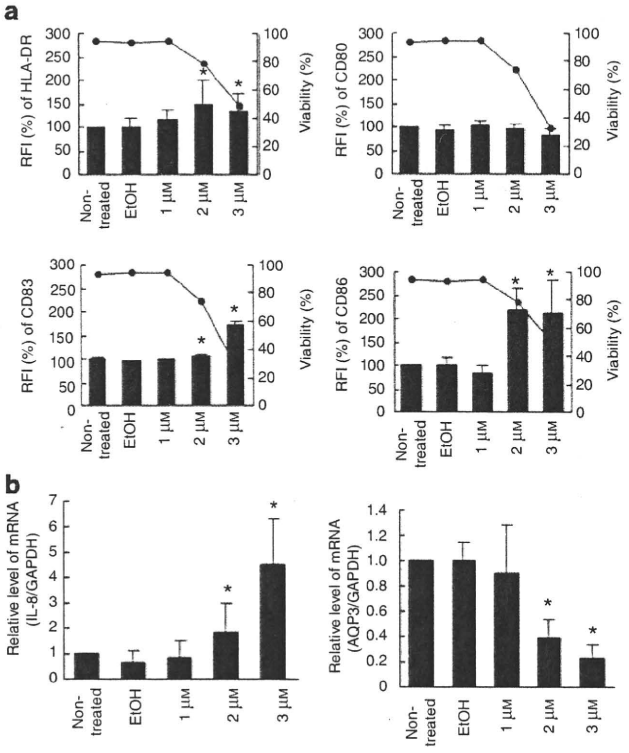

Figure 3. CuPhen induces the maturation of MoDCs. (**a**) After 24 hours treatment with three different concentrations of CuPhen, the expression of HLA-DR, CD80, CD83, and CD86 antigen by MoDCs was examined by flow cytometry. Summarized data from five different experiments are shown. The mean ± SEM of RFI is shown by black bars. A line chart shows cell viability. Asterisks indicate significance ($*P<0.05$) for the difference between stimulated cells and the vehicle-treated control. (**b**) After 6 hours of treatment, IL-8 and aquaporin-3 mRNA expressions were examined by real-time PCR. Summarized data from three different experiments are shown. The mean ± SEM of the relative level of IL-8 mRNA and aquaporin-3 mRNA is shown. Asterisks indicate significance ($*P<0.05$) for the difference between stimulated cells and the vehicle-treated control. RFI, relative fluorescence intensity.

GSH, as suggested by experiments with inhibitors of GSH synthesis or those with the D-stereoisomer of NAC (D-NAC) that cannot be converted to GSH (reviewed by Laragione *et al.* (2003)). Indeed, in this study, we showed that NAC significantly increased the cell surface thiols of MoDCs, and suppressed the phosphorylation of p38 MAPK and MoDC maturation induced by CuPhen. These data suggest that the inhibitory effects of NAC on MoDC maturation by sensitizers are at least partially mediated by its thiol-disulfide exchange activity as a reductant.

The cytoplasm represents a reducing environment, where most of the protein cysteines are in a reduced state owing to the high level of intracellular GSH (Hwang *et al.*, 1992); the extracellular environment is highly oxidizing and most known secreted proteins are very rich in disulfides (Thornton, 1981). Proteins on the cell membrane are at the interface between these two compartments and may have a key role as sensors of the environmental redox state, as their location makes them particularly sensitive to exogenous oxidants or reductants (Laragione *et al.*, 2006). Our current study showing that sensitizers oxidize cell surface thiols, causing the phosphorylation of p38 MAPK and activation of MoDCs, which are suppressed by a p38 MAPK inhibitor, seems to support this notion; that is, DCs sense sensitizers through the oxidation of cell surface thiols and transduce the signal into the phosphorylation of p38 MAPK that is well known to have a crucial role in DC maturation. Indeed, when we applied DNCB to the mouse skin, LC reduced their cell surface thiols, which suggests that sensitizers trigger LC maturation through the oxidation of cell surface thiols.

Interestingly, CuPhen also phosphorylated p42/44 ERKs. Recently, the concomitant phosphorylation of both p38 MAPK and p42/44 ERKs by reactive oxygen species have been shown through the analysis of the effects of cigarette smoke extract on DCs (Kroening *et al.*, 2008). Therefore, our study suggests that the oxidation of cell surface thiols can phosphorylate both p38 MAPK and p42/44 ERKs. In contrast to the positive role of p38 MAPK in DC maturation, which has been confirmed by a recent elegant study using a dominant active form of MAPK kinase 6, a direct upstream kinase of p38 MAPK (Jorgl *et al.*, 2007), several studies suggested the negative role of p42/44 ERKs in DC maturation, such as the upregulation of IL-12p40 and CCR7 (Li *et al.*, 2007; Kroening *et al.*, 2008). We have also reported that the suppression of p42/44 ERKs by PB98059 rather augmented CD86 expression by sensitizer-stimulated MoDCs, whereas the suppression of p38 MAPK by SB203580 significantly suppressed it (Aiba *et al.*, 2000). These studies suggest the negative role of p42/44 ERKs in DC maturation. Therefore, the role of the phosphorylation of p42/44 ERKs on CuPhen-induced DC maturation remains to be determined.

On the other hand, in contrast to several papers (Arrighi *et al.*, 2001; Aiba *et al.*, 2003; Boisleve *et al.*, 2004) showing the phosphorylation of SAPK/JNK by haptens, CuPhen did not phosphorylate SAPK/JNK. Recently, Handley *et al.* (2005) have reported that hydrogen peroxide at low concentrations phosphorylates p38 MAPK more strongly than SAPK/JNK, whereas it phosphorylates both p38 MAPK and SAPK/JNK in the same magnitude at higher concentrations. These data suggest that there is a hierarchic activation of SAPK/JNK and p38 MAPK, in which incremental reactive oxygen species stimulation sequentially activates p38 MAPK and SAPK/JNK. The lack of SAPK/JNK phosphorylation by CuPhen-treated MoDCs suggests that CuPhen did not activate MoDCs to a level sufficient to stimulate SAPK/JNK. In addition, Thoren *et al.* (2007) have shown that MoDCs have a unique capacity to neutralize extracellular oxygen radials and express higher levels of cell surface thiols than monocytes, which suggests that MoDCs are less sensitive to extracellular oxidative stress.

Finally, as many previously unknown chemicals that are likely to enter into contact with the skin are synthesized every day, it is essential to be able to predict their sensitizing potential. Accordingly, one of the goals of the research on the mechanism of allergic contact dermatitis is to develop non-animal test methods for skin sensitization testing. Several possible methods using DCs have been reported (reviewed by Ryan *et al.* (2007)). In these *in vitro* tests,

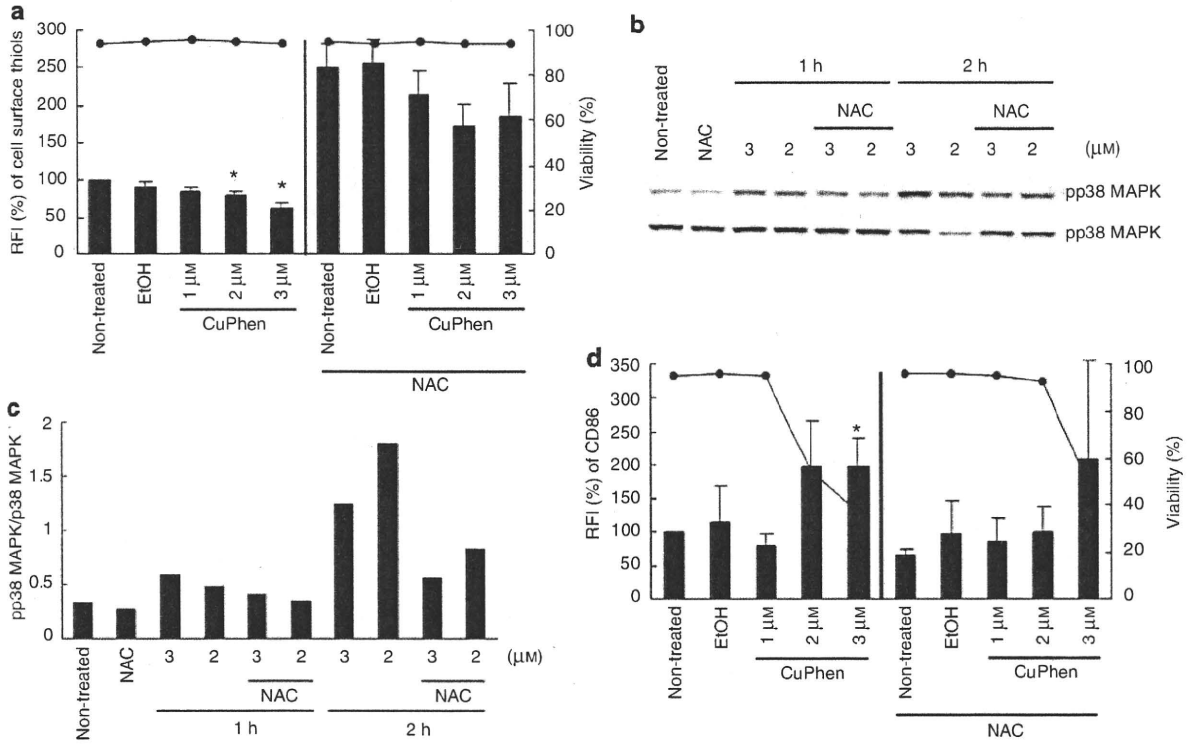

Figure 4. The pretreatment of NAC significantly increases cell surface thiols of MoDCs and suppresses the effects of CuPhen on MoDCs. To examine the effects of the antioxidant NAC, MoDCs were pretreated with 25 mM NAC for 30 minutes, washed with the culture medium, and stimulated by CuPhen. (**a**) After 2 hours treatment with CuPhen, the cell surface thiols were quantified by flow cytometry using thiol-reactive Alex Fluor 488 C5 maleimide. The mean ± SEM of RFI for cell surface thiols from three independent experiments is shown. Asterisks indicate significance (*$P<0.05$) for the difference between stimulated cells and the non-treated control. (**b**) After 1 hour or 2 hours treatment with CuPhen, the phosphorylation of p38 MAPK was examined by western blotting using anti-pp38 MAPK antibody. As a control to confirm that equal amounts of protein were loaded to the gel, total p38 MAPK is also shown. (**c**) To show the relative ratio of phosphorylated p38 MAPK *versus* total p38 MAPK, the optical densities of the signals were measured with NIH image. Shown are representative data from two different experiments. (**d**) After 24 hours treatment, the expression of CD86 antigen by MoDCs was examined by flow cytometry. Summarized data from three different experiments are shown. The mean ± SEM of RFI is shown by black bars. A line chart shows cell viability. Asterisks indicate significance (*$P<0.05$) for the difference between stimulated cells and the vehicle-treated control. RFI, relative fluorescence intensity.

the chemicals used to stimulate DCs or other cell lines are usually used at sublethal concentrations. Therefore, they may release ATP that stimulates DCs, as shown by Mizumoto *et al.* (2003). In this study, we clearly showed that ATP did not affect the cell surface thiols of MoDCs, which suggests that an assessment of cell surface thiols may be able to discriminate the stimulation by sensitizers from that by nonspecific signals of ATP. On the basis of this concept, we have developed a previously unreported *in vitro* skin sensitization test, in which we evaluate the changes of cell surface thiols on human monocyte cell line, THP-1 cells, after chemical treatment as a biomarker for skin sensitization (Suzuki *et al.*, 2009). It is clearly necessary to examine the effects of large numbers of chemicals, including haptens, prohaptens, and irritants, on the cell surface thiols of MoDCs or THP-1 to determine the possibility and limitations of this method as a non-animal test method for skin sensitizing testing.

MATERIALS AND METHODS

Media and reagents

The medium used in this study was RPMI-1640, including 25 mM Hepes buffer (Sigma-Aldrich, St Louis, MO) supplemented with 2 mM L-glutamine, 1 mM sodium pyruvate, 1% penicillin, streptomycin, and fungizone antibiotic solution (Sigma), and 10% fetal calf serum (Bioserum, Canterbury, Victoria, Australia) (complete medium). MACS colloidal supermagnetic microbeads conjugated with anti-human CD14 mAb (CD14 microbeads) were purchased from Miltenyi Biotec (Sunnyvale, CA). Recombinant human GM-CSF and recombinant human IL-4 were purchased from PeproTech (London, UK). The buffer used for the purification of $CD14^+$ monocytes from peripheral blood mononuclear cells was phosphate-buffered saline (PBS) supplemented with 1% BSA (less than 1 ng ml^{-1} of detectable endotoxin) (Sigma) and 5 mM EDTA (MACS buffer). Cu(II)SO_4, 1,10-phenanthroline (Sigma), DNCB, dephencyprone, $NiSO_4$, SDS (Sigma), formalin (HCHO), ATP (WAKO Pure Chemicals, Osaka, Japan), and squaric acid dibutyl ester (Tokyo Kasei Kogyo, Tokyo, Japan) were used for the stimulation of MoDCs. CuPhen was prepared by dissolving Cu(II)SO_4 and 1,10-phenanthroline (Sigma) in a 4:1 water/ethanol solution. $NiSO_4$, HCHO, SDS, and ATP were solubilized in distilled water, whereas DNCB, dephencyprone, and squaric acid dibutyl ester were solubilized inDMSO (Sigma). The final concentration of DMSO was always less than 0.1% and cultures of MoDCs with 0.1% DMSO were also examined as control. The antioxidant NAC, and p38 MAPK inhibitor

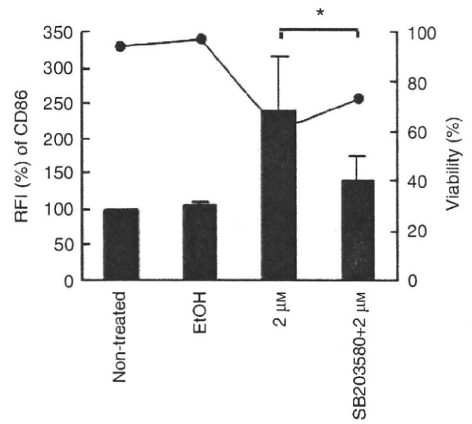

Figure 5. The treatment of SB203580 suppresses the augmentation of CD86 by CuPhen-treated MoDCs. To examine the effects of SB203580, we added 30 μM SB203580 to the culture of MoDCs 1 hour before stimulation by CuPhen and stimulated them using CuPhen. After 24 hours stimulation, the expression of CD86 antigen by MoDCs was examined by flow cytometry. Summarized data from three different experiments are shown. The mean ± SEM of RFI is shown by black bars. A line chart shows cell viability. Asterisks indicate significance ($*P<0.05$) for the difference between stimulated cells and the vehicle-treated control. RFI, relative fluorescence intensity.

SB203580 hydrochloride were purchased from Sigma and Calbiochem (San Diego, CA), respectively, and solubilized in distilled water, and then the pH was adjusted to 7.4. The endotoxin content of the final dilution used was $<30\,pg\,ml^{-1}$, as determined by the Limulus amebocyte lysate assay (Seikagaku, Tokyo, Japan).

We used the following mAbs for immunostaining: FITC-conjugated-anti-HLA-DR, FITC-conjugated-anti-CD80, phycoerythrin(PE)-conjugated-anti-CD86 (BD Pharmingen, San Diego, CA), PE-conjugated-anti-CD83 (Beckman Coulter, Fullerton, CA), FITC or PE-conjugated isotype-matched mouse control Abs (IgG1, IgG2a, and IgG2b), and PE-conjugated anti-phospho-p38 MAPK (T180/Y182) Ab (BD Pharmingen). This study was approved by the ethics committee of Shiseido Research Center, Yokohama, Japan and the ethics committee of Tohoku University Graduate School of Medicine, Sendai, Japan, and adhered to the guidelines set forth by the Helsinki protocol. All the subjects gave informed consent before the examinations.

Culture of MoDCs from peripheral blood monocytes and chemical treatment with sensitizers

Peripheral blood mononuclear cells were isolated from heparinized fresh leukocyte-enriched buffy coats from different donors using Lymphoprep (Axis-Shield PoC As, Oslo, Norway). After several washes with PBS, 1×10^8 peripheral blood mononuclear cells were treated with 200 μl of CD14 microbeads in 800 μl of MACS buffer at 4 °C for 30 minutes. After washing with MACS buffer, the cells coated with CD14 microbeads were separated by a magnetic cell separator, MACS (Miltenyi Biotech), according to the manufacturer's protocol. Before culturing, we examined the percentage of $CD14^+$ cells in these preparations by flow cytometry and used cell specimens containing more than 98% $CD14^+$ cells in the experiments.

$CD14^+$ monocytes (2×10^6 per ml) were cultured in complete medium containing $100\,ng\,ml^{-1}$ of recombinant human GM-CSF and $100\,ng\,ml^{-1}$ of recombinant human IL-4 for 6 days. One-half of the culture medium was changed on days 3 and 6. On the day 6, the cells were treated with different concentrations of DNCB, dephencyprone, squaric acid dibutyl ester, $NiSO_4$, HCHO, SDS, or ATP. After 2 hours, the cell surface thiols of these cells were examined.

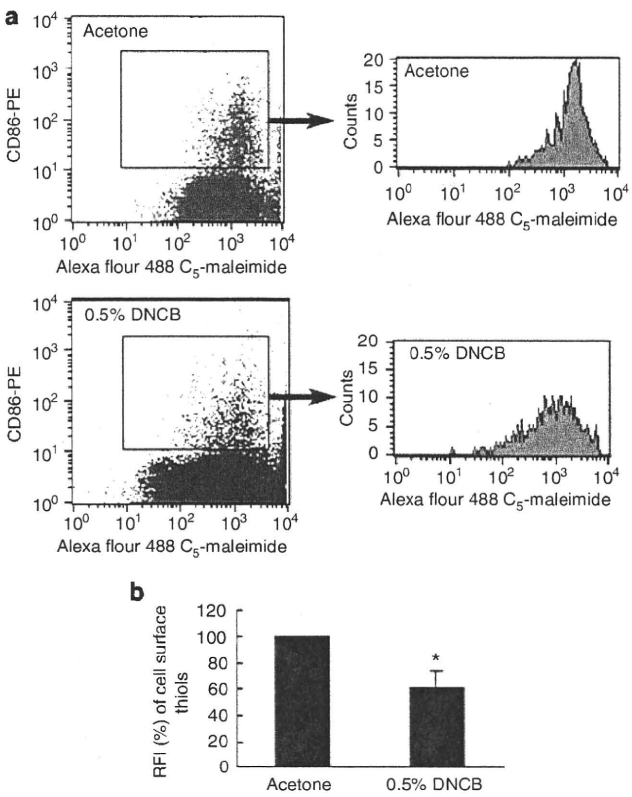

Figure 6. Epidermal langerhans cells decrease cell surface thiols after epicutaneous application of DNCB. The freshly shaved abdomens of BALB/c mice were painted with 100 μl of 0.5% of DNCB. After 2 hours, epidermal cell suspensions were prepared from the applied skin. These cell suspensions were stained with PE-conjugated anti-CD86 antibody and Alexa fluor 488 C_5 maleimide. The cell surface thiols of $CD86^+$ epidermal cells were compared between DNCB-treated mice and vehicle-treated mice. A representative flow cytometry (**a**) and the summarized data from three different experiments (**b**) are shown. The mean ± SEM of RFI is shown by black bars. Asterisk indicates significance ($*P<0.05$) for the difference between stimulated cells and the vehicle-treated control. RFI, relative fluorescence intensity.

Stimulation of MoDCs with CuPhen in the presence or absence of NAC or SB203580

Monocyte-derived DCs were treated with various concentrations of CuPhen for different time periods. In some experiments, to examine the effects of the antioxidant NAC, MoDCs were exposed to 25 mM NAC for 30 minutes, washed with the culture medium, and stimulated by the chemicals. To examine the effects of p38 MAPK inhibitor, cells were treated with 30 μM of SB203580, as we have reported previously (Aiba *et al.*, 2003).

Flow cytometry for MoDCs

To stain cell surface thiols, MoDCs were recovered from the culture, washed with PBS twice, and then incubated with 100 μl of Alexa Fluor 488 C_5 maleimide (Invitrogen) PBS solution (10 μM) for 30 minutes at 37 °C. To analyze the intracellular expression of phospho-p38

MAPK, we permeabilized the cells using Fix & Perm reagents (Caltag Laboratories, Burlingame, CA) according to the manufacturer's protocol, and cell staining was performed using a PE-conjugated anti-phospho-p38 MAPK (T 180/Y 182). For immunophenotyping, cell staining was performed using FITC-conjugated-anti-HLA-DR, FITC-conjugated-anti-CD54, FITC-conjugated-anti-CD80, PE-conjugated-anti-CD86, PE-conjugated-anti-CD83 Ab, and FITC or PE-conjugated isotype-matched mouse control Abs ($10\,\mu g\,ml^{-1}$). After washing with FACS buffer, the cells were analyzed by FACScan using CellQuest software (Becton-Dickinson, San Jose, CA). Dead cells were gated out after staining with $0.5\,mg\,ml^{-1}$ propidium iodide solution for non-permeabilized cells. In some experiments, relative fluorescence intensity (RFI) was calculated by using the following formula: RFI (%) = (Mean fluorescence intensity (MFI) of chemical-treated cells/MFI of vehicle control cells) × 100. To calculate cell viability, dead cells were counted as propidium iodide(+) cells and viability (%) was calculated by dividing the numbers of dead cells by those of propidium iodide(−) living cells ± dead cells.

Analysis of phospho-MAPKs and phospho-IκB by immunoblotting

Monocyte-derived DCs were either unstimulated or stimulated with CuPhen for 1 or 2 hours. To examine the effects of NAC or p38 MAPK inhibitor, cells were treated with 25 mM NAC or 30 μM of SB203580, as we have described above. The cells were washed twice in cold PBS and resuspended in 250 μl of lysis buffer (1% Nonidet P-40, 20 mM Tris-HCl (pH 8.0), 137 μM NaCl, 10% glycerol, 2 mM EDTA, $10\,\mu g\,ml^{-1}$ leupeptin, $10\,\mu g\,ml^{-1}$ aprotinin, 1 mM phenylmethanesulfonyl fluoride, and 1 mM sodium orthovanadate). The nuclei and the insoluble cell debris were removed by centrifugation at 4 °C for 10 minutes at 14,000 × *g*. The postnuclear extracts were collected and used as the total cell lysates. The total cell lysates were suspended in 2 × SDS sample buffer (313 mM Tris-HCl (pH 6.8), 10% SDS, 2-mercaptoethanol, 50% glycerol, and 0.01% bromophenol blue) and heated at 95 °C for 3 minutes. The protein samples were subjected to SDS-PAGE and transferred onto nitrocellulose membranes. The nonspecific Ab binding sites on the membranes were blocked with 1% BSA, 0.01% Tween20 in saline (10 mM Tris-HCl (pH 7.4) 100 mM NaCl) for 20 minutes at 37 °C. Immunoblotting of phosphorylated p42/44 ERKs, SAPK/JNK, p38 MAPK, or IκB was performed using p42/44 ERKs, SAPK/JNK, p38 MAPK, or IκB immunoblotting kits purchased from Cell Signaling Technology (Beverly, MA), respectively, as we have reported previously (Aiba *et al.*, 2003). Briefly, the membranes were incubated for 16 hours at 4 °C with rabbit polyclonal Abs to anti-tyrosine phosphorylated p42/44 ERKs, SAPK/JNK, p38 MAPK, or anti-serine (Ser32/36) phosphorylated IκB, washed for 15 minutes, and incubated with horseradish peroxidase-conjugated secondary Abs for 1 hour at room temperature. Blots were visualized by enhanced chemiluminescence. To ensure that there were similar amounts of MAPKs or IkB in each sample, the same membranes were stripped off, reprobed with Abs to p42/44 ERKs, SAPK/JNK, p38 MAPK, or IkB and developed with horseradish peroxidase-conjugated secondary Abs by enhanced chemiluminescence.

Quantitative real-time reverse transcription PCR

Quantitative, fluorescent PCR was performed using the TaqMan system (ABI 7700: Applied Biosystems, Foster City, CA). Sequences for human GAPDH, IL-8, and AQP3 were obtained from GenBank. We chose forward and reverse primers to span exon-intron boundaries. TaqMan probes were chosen to be used with these primers using Primer Express version. 1.0 (Applied Biosystems). Forward and reverse primers were made by Operon (Nihon Gene Research Laboratories, Sendai, Japan), whereas TaqMan probes were made by Applied Biosystems. The primers used were as follows: IL-8, forward 5′-GTGTGTAAACATGACTTCCAAGCTG-3′, reverse 5′-TCTTTAGCACTCCTTGGCAAAAC-3′; AQP3, forward 5′-CCCAT CGTGTCCCCA-3′, reverse 5′-GCCGATCATCAGCTGGTACA-3′; GAPDH, forward 5′-GAAGGTGAAGGTCGGAGTC-3′, reverse 5′-GAA GATGGTGATGGGATTTC-3′. Probes, 5′-(FAM490-labeled)-3′(tetra-methylrhodamine-labeled), were as follows: IL-8, 5′-TGATTTCTGC AGCTCTGTGTCAAGGTGC-3′; AQP3, 5′-TGATTTCTGCAGCTCTG TGTGAAGGTGC-3′; GAPDH, 5′-TGGCAAATTCCATGGGACCGT CA-3′. RNA was extracted by using the guanidinium thiocyanate method described by the manufacturer (ISOGEN; Nippon gene, Toyama, Japan) from MoDCs either unstimulated or stimulated using CuPhen for 6 hours. First strand cDNA was synthesized from total RNA extracted in RNase-free conditions. cDNA was obtained from total RNA using TaKaRa RNA PCR kit (AMV) (Takara Biochemicals, Osaka, Japan), as described by the manufacturer's protocol. PCR for GAPDH, IL-8, and AQP3 were performed in triplicate in 30 μl total reaction volumes using 66 nM TaqMan probe, 400 nM forward primers, 400 nM reverse primers, and 2 × TaqMan universal PCR Master (Applied Biosystems). Thermal cycling was performed for 2 minutes at 50 °C for depleting contaminated RNA, 10 minutes denaturation at 95 °C, followed by 40 cycles at 95 °C for 15 seconds, and at 60 °C for 1 minute in the ABI Prism 7700 detection system (Applied Biosystems). The levels of cDNA for GAPDH, IL-8, and AQP3 generated from cellular RNA were calculated by using standard curves generated with bona fide human cDNAs for GAPDH, IL-8, or AQP3, in which there was linear relationship between the number of cycles required to exceed the threshold and the number of copies of cDNA added.

Mice

BALB/c mice were obtained from Japan SLC (Shizuoka, Japan). Female mice, 8 weeks old, were used. The study was approved by the Animal Research Committee of Tohoku University and the ethics committee of Shiseido Research Center in accordance with the National Research Council Guidelines and the National Institute of Health.

Preparation of murine epidermal cell suspensions

In total 100 μl of 0.5% DNCB in acetone:olive oil (4:1) was applied to the freshly shaved abdomen of mice. Control mice were painted on the shaved abdomen with 100 μl of the vehicle. After 2 hours, skin sheets from abdomens were floated in 0.1% trypsin in PBS (pH 7.4) for 30 minutes at 37 °C. The epidermis was peeled in 0.1% DNase I solution (0.05% DNase I in PBS supplemented with 25% fetal calf serum), injected vigorously, and filtered through nylon mesh.

Flow cytometry of murine epidermal cell suspensions

Murine epidermal cells were washed with FACS buffer and then incubated with 100 μl of Alexa fluor 488 C_5 maleimide PBS solution (10 μM) for 30 minutes at 37 °C. After washing with FACS buffer, the cells were stained using a PE-conjugated anti-mouse CD86 ab. After washing with FACS buffer, the cells were analyzed by FACScalibur

using CellQuest software (Becton-Dickinson). Viable cells were identified by 7-AAD (BD Pharmingen) uptake.

Statistical analysis

Data were presented as mean ± SEM, and the statistical significance was analyzed using paired Student's *t*-test and considered to be significant at $P<0.05$. To examine the correlation between the cell surface thiol expression and phosphorylation of p38 MAPK, we calculated all the data from MoDCs stimulated with various concentrations of chemicals by Pearson's correlation coefficients.

CONFLICT OF INTEREST

The authors state no conflict of interest.

ACKNOWLEDGMENTS

This study was supported in part by the 21st COE program of Tohoku University, by New Energy and Industrial Technology Development Organization, and by a grant-in-aid for scientific research from the Japan Society for the Promotion of Science (17790749).

REFERENCES

Aiba S, Katz SI (1990) Phenotypic and functional characteristics of *in vivo*-activated Langerhans cells. *J Immunol* 145:2791–6

Aiba S, Manome H, Nakagawa S, Mollah ZU, Mizuashi M, Ohtani T *et al.* (2003) p38 mitogen-activated protein kinase and extracellular signal-regulated kinases play distinct roles in the activation of dendritic cells by two representative haptens, $NiCl_2$ and DNCB. *J Invest Dermatol* 120:390–8

Aiba S, Manome H, Yoshino Y, Tagami H (2000) *In vitro* treatment of human TGF-beta1-treated monocyte-derived dendritic cells with haptens can induce the phenotypic and functional changes similar to epidermal Langerhans cells in the initiation phase of allergic contact sensitivity reaction. *Immunol* 101:68–75

Aiba S, Terunuma A, Manome H, Tagami H (1997) Dendritic cells differently respond to haptens and irritants by their production of cytokines and expression of co-stimulatory molecules. *Eur J Immunol* 27:3031–8

Arrighi JF, Rebsamen M, Rousset F, Kindler V, Hauser C (2001) A critical role for p38 mitogen-activated protein kinase in the maturation of human blood-derived dendritic cells induced by lipopolysaccharide, TNF-alpha, and contact sensitizers. *J Immunol* 166:3837–45

Boisleve F, Kerdine-Romer S, Rougier-Larzat N, Pallardy M (2004) Nickel and DNCB induce CCR7 expression on human dendritic cells through different signalling pathways: role of TNF-alpha and MAPK. *J Invest Dermatol* 123:494–502

Brand P, Plochmann S, Valk E, Zahn S, Saloga J, Knop J *et al.* (2002) Activation and translocation of p38 mitogen-activated protein kinase after stimulation of monocytes with contact sensitizers. *J Invest Dermatol* 119:99–106

Ciriolo MR, Paci M, Sette M, De Martino A, Bozzi A, Rotilio G (1993) Transduction of reducing power across the plasma membrane by reduced glutathione. A 1H-NMR spin-echo study of intact human erythrocytes. *Eur J Biochem* 215:711–8

Coutant KD, de Fraissinette AB, Cordier A, Ulrich P (1999) Modulation of the activity of human monocyte-derived dendritic cells by chemical haptens, a metal allergen, and a staphylococcal superantigen. *Toxicol Sci* 52:189–98

de Baey A, Lanzavecchia A (2000) The role of aquaporins in dendritic cell macropinocytosis. *J Exp Med* 191:743–8

De Smedt AC, Van Den Heuvel RL, Zwi Berneman N, Schoeters GE (2001) Modulation of phenotype, cytokine production and stimulatory function of CD34+-derived DC by NiCl(2) and SDS. *Toxicol In Vitro* 15:319–25

Duncan DD, Lawrence DA (1989) Differential lymphocyte growth-modifying effects of oxidants: changes in cytosolic Ca+2. *Toxicol Appl Pharmacol* 100:485–97

Filomeni G, Rotilio G, Ciriolo MR (2003) Glutathione disulfide induces apoptosis in U937 cells by a redox-mediated p38 MAP kinase pathway. *FASEB J* 17:64–6

Handley ME, Thakker M, Pollara G, Chain BM, Katz DR (2005) JNK activation limits dendritic cell maturation in response to reactive oxygen species by the induction of apoptosis. *Free Radic Biol Med* 38:1637–52

Hirota M, Suzuki M, Hagino S, Kagatani S, Sasaki Y, Aiba S *et al.* (2009) Modification of cell-surface thiols elicits activation of human monocytic cell line THP-1: possible involvement in effect of haptens 2,4-dinitrochlorobenzene and nickel sulfate. *J Toxicol Sci* 34:139–50

Hwang C, Sinskey AJ, Lodish HF (1992) Oxidized redox state of glutathione in the endoplasmic reticulum. *Science* 257:1496–502

Jorgl A, Platzer B, Taschner S, Heinz LX, Hocher B, Reisner PM *et al.* (2007) Human Langerhans-cell activation triggered *in vitro* by conditionally expressed MKK6 is counterregulated by the downstream effector RelB. *Blood* 109:185–93

Kroening PR, Barnes TW, Pease L, Limper A, Kita H, Vassallo R (2008) Cigarette smoke-induced oxidative stress suppresses generation of dendritic cell IL-12 and IL-23 through ERK-dependent pathways. *J Immunol* 181:1536–47

Laragione T, Bonetto V, Casoni F, Massignan T, Bianchi G, Gianazza E *et al.* (2003) Redox regulation of surface protein thiols: identification of integrin alpha-4 as a molecular target by using redox proteomics. *Proc Natl Acad Sci USA* 100:14737–41

Laragione T, Gianazza E, Tonelli R, Bigini P, Mennini T, Casoni F *et al.* (2006) Regulation of redox-sensitive exofacial protein thiols in CHO cells. *Biol Chem* 387:1371–6

Lawrence DA, Song R, Weber P (1996) Surface thiols of human lymphocytes and their changes after *in vitro* and *in vivo* activation. *J Leukoc Biol* 60:611–8

Li G, Basu S, Han MK, Kim YJ, Broxmeyer HE (2007) Influence of ERK activation on decreased chemotaxis of mature human cord blood monocyte-derived dendritic cells to CCL19 and CXCL12. *Blood* 109:3173–6

Mizuashi M, Ohtani T, Nakagawa S, Aiba S (2005) Redox imbalance induced by contact sensitizers triggers the maturation of dendritic cells. *J Invest Dermatol* 124:579–86

Mizumoto N, Mummert ME, Shalhevet D, Takashima A (2003) Keratinocyte ATP release assay for testing skin-irritating potentials of structurally diverse chemicals. *J Invest Dermatol* 121:1066–72

Ozawa H, Nakagawa S, Tagami H, Aiba S (1996) Interleukin-1 beta and granulocyte-macrophage colony-stimulating factor mediate Langerhans cell maturation differently. *J Invest Dermatol* 106:441–5

Ryan CA, Kimber I, Basketter DA, Pallardy M, Gildea LA, Gerberick GF (2007) Dendritic cells and skin sensitization: biological roles and uses in hazard identification. *Toxicol Appl Pharmacol* 221:384–94

Staquet MJ, Sportouch M, Jacquet C, Schmitt D, Guesnet J, Peguet-Navarro J (2004) Moderate skin sensitizers can induce phenotypic changes on *in vitro* generated dendritic cells. *Toxicol In Vitro* 18:493–500

Suzuki M, Hirota M, Hagino S, Itagaki H, Aiba S (2009) Evaluation of changes of cell-surface thiols as a new biomarker for *in vitro* sensitization test. *Toxicology In Vitro* 23:687–96

Tanaka T, Nakamura H, Yodoi J, Bloom ET (2005) Redox regulation of the signaling pathways leading to eNOS phosphorylation. *Free Radic Biol Med* 38:1231–42

Thoren FB, Betten A, Romero AI, Hellstrand K (2007) Cutting edge: antioxidative properties of myeloid dendritic cells: protection of T cells and NK cells from oxygen radical-induced inactivation and apoptosis. *J Immunol* 179:21–5

Thornton JM (1981) Disulphide bridges in globular proteins. *J Mol Biol* 151:261–87

Tuschl H, Kovac R, Weber E (2000) The expression of surface markers on dendritic cells as indicators for the sensitizing potential of chemicals. *Toxicol In Vitro* 14:541–9

Zafarullah M, Li WQ, Sylvester J, Ahmad M (2003) Molecular mechanisms of *N*-acetylcysteine actions. *Cell Mol Life Sci* 60:6–20

ORIGINAL ARTICLE

Utilization of Reconstructed Cultured Human Skin Models as an Alternative Skin for Permeation Studies of Chemical Compounds

Satoshi Kano, Hiroaki Todo, Kenichi Sugie, Hidenori Fujimoto, Keiichi Nakada, Yoshihiro Tokudome, Fumie Hashimoto and Kenji Sugibayashi

Faculty of Pharmaceutical Sciences, Josai University, Saitama, Japan

Abstract

Two reconstructed human skin models, Episkin^{SM} and EpiDerm^{TM}, have been approved as alternative membranes for skin corrosive/irritation experiments due to their close correlation with animal skin. Such reconstructed human skin models were evaluated as alternative membranes for skin permeation experiments. Seven drugs with different lipophilicities and almost the same molecular weight were used as test penetrants. Relationships were investigated between permeability coefficients (P values) of the seven drugs through six kinds of reconstructed cultured human skin models and human skin. A fairly good relationship in P values was observed between TESTSKIN^{TM} LSE-high (LSE-high) or EpiDerm^{TM} and human skin, suggesting that these reconstructed human skin models could be used as alternative membranes for skin permeation experiments. However, the partition parameter, KL, and diffusion parameter, DL^{-2} in these reconstructed human skin models were different to those of human skin. Especially, KL values in reconstructed human skin models were very different to those in human skin, even for LSE-high and EpiDerm^{TM}. Therefore, suitable reconstructed human skin models should be carefully selected on a case by case basis.

Key words: *reconstructed human skin models, skin permeation, alternative membrane. skin corrosive/irritation*

Introduction

Excised human cadaver skin and experimental animal skins have been widely used for *in vitro* skin permeation- and skin corrosive/irritation-experiments with chemical compounds. Recently, reconstructed cultured human skin models (cultured skin models) have been seen as a promising alternative membrane for human and animal skins. The European Center for the Validation of Alternative Methods (ECVAM) approves Episkin^{SM} and EpiDerm^{TM} as alternative animal membranes in skin corrosive experiments. Now, various kinds of cultured skin models such as living human skin equivalent TESTSKIN^{TM} SE-high, LabCyte EPI-Model, Vitrolife-skin and Neoderm-E, are available in Japan in addition to Episkin^{SM} and EpiDerm^{TM}. Many reports have revealed the usefulness of such cultured human skin models in skin permeation experiments with chemical compounds, as well as skin corrosive/irritation experiments (Netzlaff *et al.*, 2007; Schmook *et al.*, 2001; Gabbanini *et al.*, 2009; Lotte *et al.*, 2002; Hammell *et al.*, 2005; Asbill *et al.*, 2000; Wagner *et al.*, 2001). These reports, however, only showed different skin permeation-time profiles or permeability coefficient (P) values of chemical compounds between excised human cadaver skin or excised animal skin and a

cultured skin model. We have already shown a 1:1 relationship in the *P* values of chemical compounds for excised human cadaver skin and hairless rat skin (Watanabe *et al.*, 2001; Morimoto *et al.*, 1992).

Generally, the *P* value of chemical compounds is the product of partition (*KL*) and diffusion parameters (DL^{-2}). The permeability parameters *KL* and DL^{-2} are closely related to the lipophilicity or transfer potential of chemical compounds, respectively, into the stratum corneum. Therefore, the *KL* and DL^{-2} profiles of different compounds represent the characteristics of each cultured human skin model in permeation experiments. In our previous report (Watanabe *et al.*, 2001), log *P* values of chemical compounds through LSE-high, a cultured human skin model, showed a fairly good relationship to those through excised cadaver human skin when seven kinds of chemicals with different physicochemical characteristics were applied to their skin. However, *P* values of chemical compounds in LSE-high were about ten-fold higher than those in excised human cadaver skin. This was due to a ten-fold higher DL^{-2} and almost the same *KL* values to those in excised human cadaver skin (Watanabe *et al.* 2001). Thus, the skin permeation parameters *KL* and DL^{-2} could aid understanding of the characteristics of cultured human skin models as an alternative membrane for skin permeation experiments.

In the present study, epidermis and dermis models, TESTSKIN™ LSE-high, Vitrolife-skin and epidermis models, EpiDerm™ 606X, LabCyte EPI-model, Neoderm-E and EpiskinSM were selected as cultured human skin models. *P* value and skin permeation parameters of chemical compounds were compared to those through excised human cadaver skin using seven kinds of chemical compounds with different lipophilicities and almost the same molecular weight. Understanding the characteristics of each cultured human skin model using *P* values would be useful to predict *P* values in human skin. Thus, this experiment could directly lead to a reduction in animal skin permeation experiments.

Theoretical

1. The relationship between P values and the n-octanol/water partition coefficient (Ko/w) of chemical compounds in excised human cadaver skin.

We (Morimoto *et al.*, 1992, Watanabe *et al.*, 2001) investigated the relationship between *P* values and the *n*-octanol/water coefficient (*K*o/w) of 30 chemical compounds. Figure 1 illustrates the relationship in excised human cadaver skin (Morimoto *et al.*, 1992, Watanabe *et al.*, 2001). A linear increase in the log *P* values in excised human cadaver skin was found by an increase in log *K*o/w of chemical compounds from log *K*o/w =1.

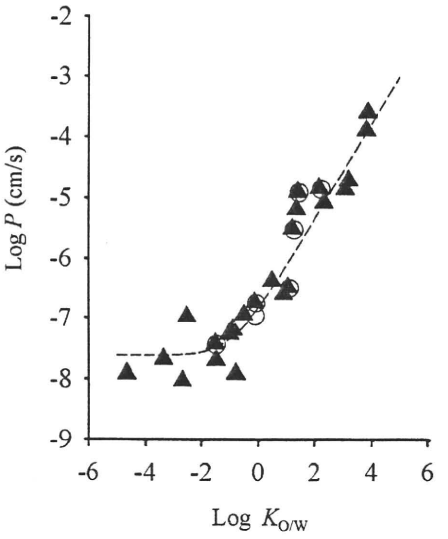

Figure 1 Relationship between log *P* values in excised human cadaver skin and log *K*o/w values of chemical compounds. Semi-solid line represents the calculated value: *P*human (cm/s) = 1.77×10^{-7} *K*ow $^{0.780}$ +2.37×10^{-8} (Morimoto *et al.*, 1992), Symbol represents observed value. Symbols:▲; values cited from Morimoto *et al.*, 1992, ○:values cited from Watanabe *et al.*, 2001.

2. Relationship between KL or DL-2 and Ko/w of chemical compounds in excised human cadaver skin.

Figure 2 illustrates double logarithmic plots of skin permeation parameters (DL^{-2} or *KL*) and the *Ko/w* of chemical compounds. Log DL^{-2} was almost constant over the present log *Ko/w* of the chemical compounds. On the other hand, log *KL* increased with an increase in log *Ko/w* and the relationship between log *Ko/w* and log *KL* was similar to that between log *P* and log *Ko/w* as shown in Fig. 1.

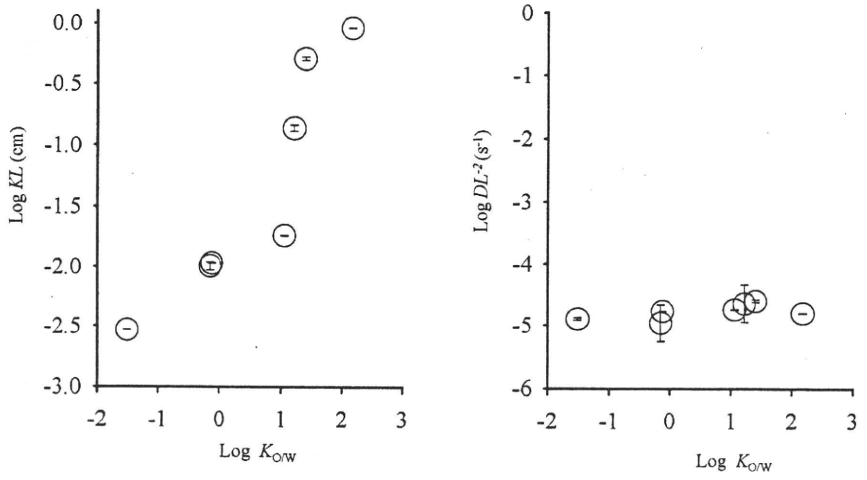

Figure 2 Relationships between log *KL* (a) and log D/L^{-2} (b) values in excised human cadaver skin and log *K*o/w values of chemical compounds. Each point represents the mean ± S.E. (n=4-6)

Table 1 Physicochemical properties of the chemical compounds

Drug	Abbreviation	Log *K*o/w	M.W.
Antipyrine	ANP	- 1.507	188
Isosorbide-5-mononitrate	ISMN	- 0.151	191
Caffeine	CAF	- 0.123	194
Aminopyrine	AMP	1.065	231
Isosorbide dinitrate	ISDN	1.225	236
Benzoic acid	BA	1.410	122
Flurbiprofen	FP	2.179	224

3. Calculation of skin permeation parameters

Each flux was calculated from the time profiles of the cumulative amount of the chemical compounds permeated through skin in skin permeation experiments, and the *P* value was calculated by a division of the steady state-flux by applied chemical compound concentration. The skin permeation-time profile was expressed by eq. 1, which comes from Fick's second law of diffusion (Scheuplein, 1967) and the lag time was calculated from the regression line from the steady state-flux region of the permeation curve. The skin permeation parameters DL^{-2} and *KL* were calculated from eq. 1 and the lag time (t_{lag}) (eq. 2), which was obtained from eq. 1 (Shah, 1993).

$$Q = KLCv\left[\frac{D}{L^2}t - \frac{1}{6} - \frac{2}{\pi^2}\sum_{n=1}^{\infty}\frac{(-1)^n}{n^2}\exp\left(-\frac{D}{L^2}n^2\pi^2 t\right)\right] \quad (1)$$

$$t_{Lag} = \frac{L^2}{6D} \quad (2)$$

$$P = (DL^{-2})\cdot(KL) \quad (3)$$

where *Q* is the cumulative amount of chemical compounds permeated, *K* is the partition coefficient, *L* is the thickness of the barrier membrane, *Cv* is the chemical compound concentration in the vehicle, *D* is diffusivity and *t* is time after application of the chemical compound on the skin. The *P* value is expressed as a product of DL^{-2} and *KL* (eq. 3).

Materials and Methods

1. Materials

Antipyrine (ANP), caffeine (CAF), aminopyrine (AMP) and benzoic acid (BA) were purchased from Wako Pure Chemical Industries, Ltd. (Osaka, Japan). Isosorbide dinitrate (ISDN) was from Sigma Aldrich Corporation (St. Louis, MO, U.S.A.) and isosorbide mononitrate (ISMN) was from Tokyo Chemical Industry Co., Ltd. (Toyko, Japan). Flurbiprofen (FP) was gifted from Lead Chemical Co., Ltd. (Toyama, Japan). Other chemicals and solvents were of reagent or HPLC grade and used without further purification. Table 1 shows the molecular weight and log

Ko/w values of these chemical compounds.

2. Reconstructed cultured human skin models

EpiDerm™ Epi606X (EpiDerm), Neoderm-E, Vitrolife-skin, LabCyte EPI-model and Episkin℠ (Episkin) were purchased from Kurabo Industries Ltd. (Osaka, Japan), Tego Science Inc. (Gumcheon-gu, Seoul, Korea), Gunze Ltd. (Kyoto, Japan), Japan Tissue Engineering Co., Ltd. (Gamagori, Aichi, Japan) and Skinethic Laboratories (St. Philippe, France), respectively. All of these models were used within 3 days of receipt.

3. Skin permeation experiment

Each cultured human skin model was carefully removed from 6 or 12 well transwells and the stratum corneum side was well rinsed with pH7.4 phosphate buffered saline (PBS). The obtained EpiDerm, Neoderm-E and Vitrolife-skin were mounted in a side by-side diffusion cell (effective diffusion area 0.95 cm^2) (Okumura *et al.*, 1989) and LabCyte EPI-model and Episkin were mounted in a Franz type diffusion cell (effective diffusion area 0. 50 cm^2). The cultured skin was hydrated with PBS over 1 hour. Then, PBS was removed and a chemical compound solution or suspension in PBS (chemical compound concentration: about two or three times solubility) was applied on the stratum corneum side and and the same volume of PBS for hydrophilic compounds (antipyrine, ISMN and caffeine) or 40% polyethylene glycol 400 for lipophilic compounds (aminopyrine, ISDN, benzoic acid and flurbiprofen) was applied to the dermal side. Skin permeation of each chemical compound was followed at 32°C by periodic sampling of 1 mL from the receiver solution. The same volume of the solvent was added to keep the volume constant. The chemical compound concentration in each sample was assayed by HPLC. Permeation results through excised human cadaver skin and TESTSKIN™ LSE-high (LSE-high) were referred to our previous report (Watanabe *et al.*, 2001).

4. HPLC conditions

Each sample was mixed with acetonitrile containing an internal standard. The solution was centrifuged (15,000 rpm, 5 min, 4°C) and 20 μL of the supernatant was injected into an HPLC system composed of an auto injector (SIL-10A, Shimadzu, Kyoto, Japan), a pump (LC-10AD, Shimadzu), a detector (SPD-10AV, Shimadzu), an integrator (SCL-10A, Shimadzu) and a reverse-phase column (Wakopak Wakosil-2 5C18HG, 4.6 mm i.d.×250 mm, Wako Pure Chemical Industries, Ltd., Osaka, Japan). The flow rate was 1.0 mL/min and the column temperature was maintained at 40°C by an oven (CTO-10AC, Shimadzu). Each data analysis was performed by Smart Chrom (KYA Technologies Corp., Tokyo, Japan). The mobile phase, internal standard and UV wavelength for detection were as follows. AMP; acetonitrile : 0.1% phosphoric acid containing 5 mM SDS=10 : 90, butyl *p*-hydroxyl benzoate, 245 nm, ISDN; acetonitrile : water=55 : 45, butyl *p*-hydroxyl benzoic acid, 245 nm, BA; acetonitrile : 50 mM potassium dihydrogen phosphate=45 : 55, ethyl *p*-hydroxyl benzoate, 245 nm, FP; acetonitrile : 0.1% phosphoric acid=50 : 50, isopropyl *p*-hydroxyl benzoate, 245 nm, respectively. ANP and CAF were detected using an absolute calculation method and mobile phase and UV wavelength for detection were as follows. ANP; acetonitrile : water=30 : 70, 254 nm, ISMN and CAF; acetonitrile : water=10 : 90, 220 nm and 254 nm, respectively.

5. Statistical analysis

Spearman's rank correlation coefficient was used to evaluate whether a good relationship was obtained between log *P* values of chemical compounds in human skin and those in cultured human skin at a 5% significance level.

Results

1. Relationship between log P values in cultured skin model and those in excised human cadaver skin.

Figure 3a-f shows a double logarithmic plot of *P* values through each cultured skin model and *Ko*/w of chemical compounds. Log *P* values in human skin are also shown in the Fig. 1 and represented by open circles. As shown in Fig. 3a, an increase in log *Ko*/w increased log *P* in LSE-high. All of the obtained log *P* values in LSE-high were about 10 times higher than those in human skin. Almost the same results were

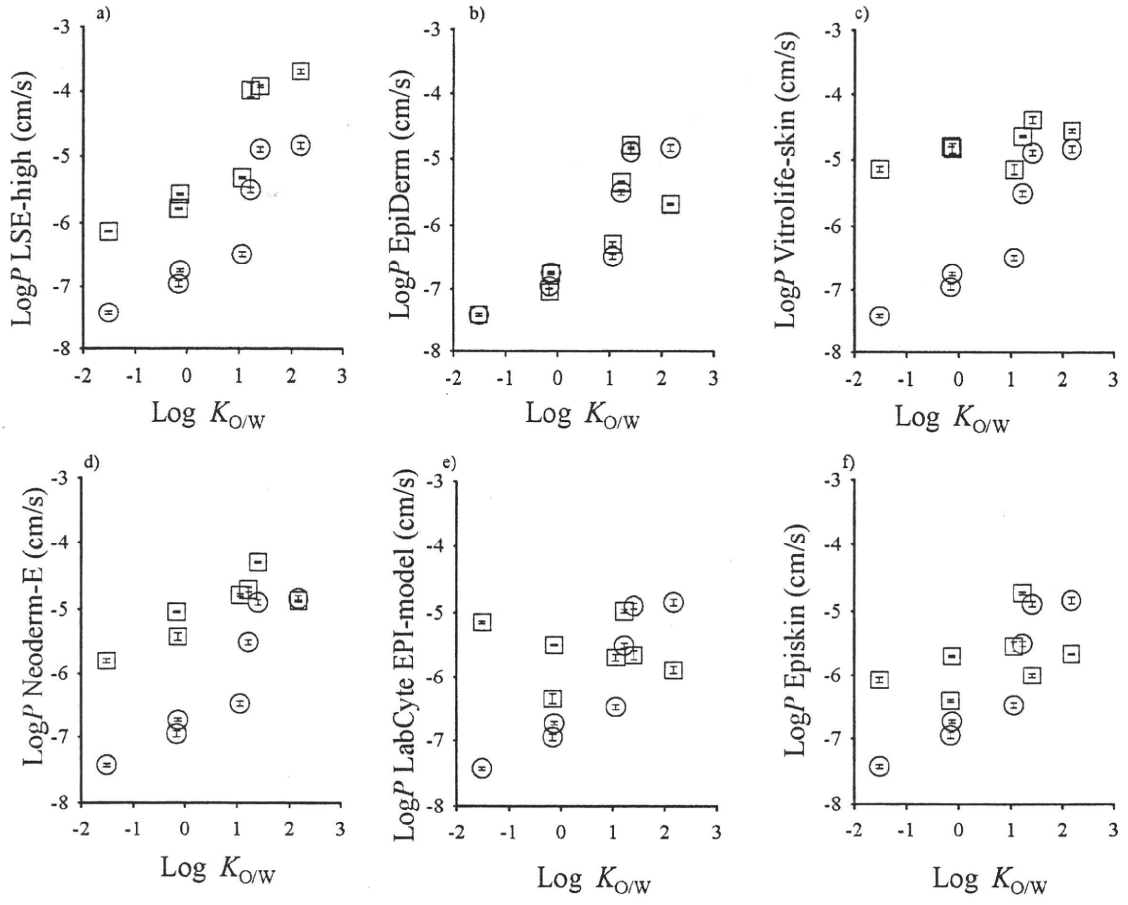

Figure 3 Relationships between log *P* values in cultured skin models and log *K*o/w values of chemical compounds. (a): LSE-high, (b): EpiDerm, (c): Vitrolife-skin, (d): Neoderm-E (e) LabCyte EPI-model and (f): Episkin. Symbols: ○; human skin, □; cultured skin model. Each point represents the mean ± S.E. (n=4-6).

found in our previous study (Watanabe *et al.*, 2001). In EpiDerm, the log *P* values of chemical compounds except for FP were almost the same values as those in human skin (Fig. 3b). The log *P* values of chemical compounds in Vitrolife-skin and Neoderm-E (Fig. 3c, d) were constant independent of log *K*o/w values, although log *P* values of BA and FP corresponded to those in excised human cadaver skin. On the other hand, the log *P* values of chemical compounds in LabCyte EPI-model and Episkin (Fig. 3e, f) were very different and no order rule was observed. The *P* value of CAF in Episkin was similar to that reported by Netzlaff *et al.* (2007). Figure 4 shows the relationships between the log *P* values of chemical compounds in cultured skin models (x-axis) and those in excised human cadaver skin (y-axis). As seen in Fig. 4a, a fairly good correlation (slope 1.0; 1:1 relationship) was observed between LSE-high and excised human cadaver skin, although log *P* values in LSE-high were about 10-folds higher than those in the excised human skin. A similar result was obtained in our previous study (Watanabe *et al.*, 2001). A fairly good correlation, Log P_{human}=1.022 × Log $P_{EpiDerm}$ - 0.202 (r = 0.9401) ($p < 0.05$), was also observed between EpiDerm and excised human cadaver skin as shown in Fig. 4b. Different to LSE-high, the log *P* values in EpiDerm were almost the same as those in excised human cadaver skin. On the other hand, in Fig. 4 c-f, the relationships between Vitrolife-skin, Neoderm-E, LabCyte EPI-model and Episkin and excised human cadaver skin in *P* values of chemical compounds were represented by the following equations; log P_{human}=2.929 × log $P_{vitrolife\text{-}skin}$ + 7.871 r= 0.8035) (no significant correlation), log P_{human}=1.688× log $P_{Neoderm\text{-}E}$ +

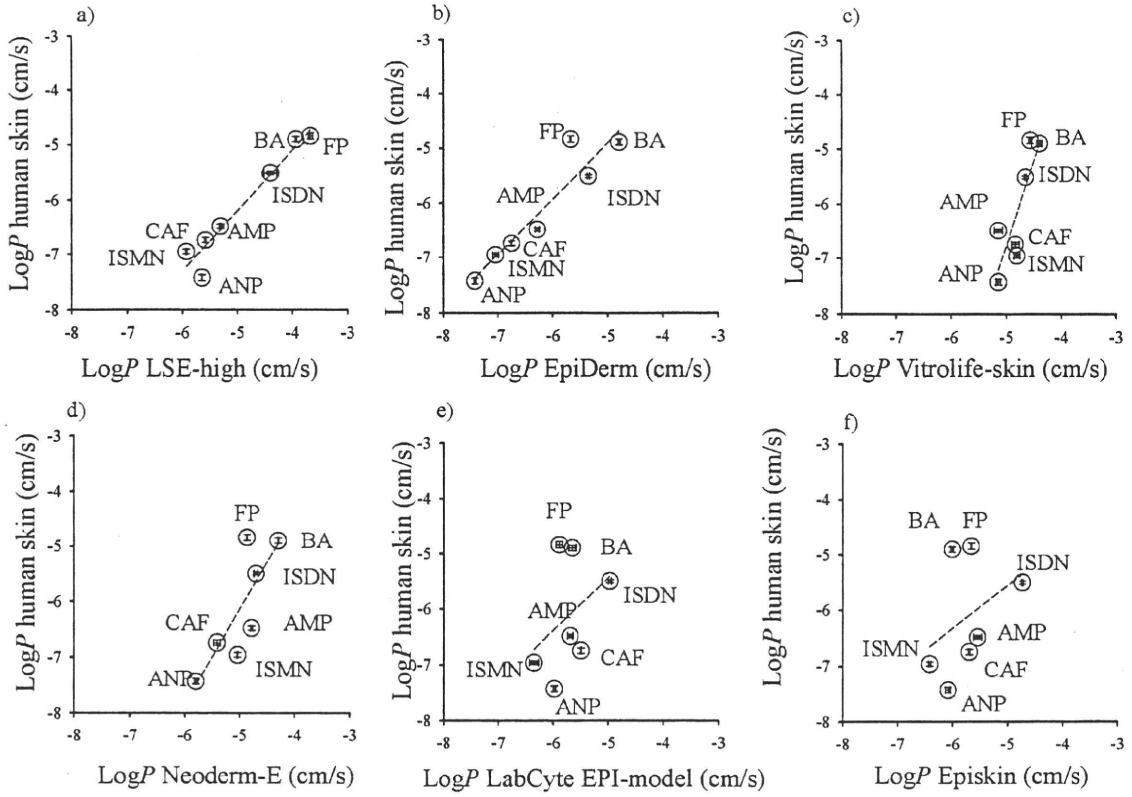

Figure 4 Relationships between log *P* values in excised human cadaver skin and log *P* values in cultured skin models. (a): LSE-high versus excised human cadaver skin, (b): EpiDerm versus excised human cadaver skin, (c): Vitrolife-skin versus excised human cadaver skin, (d): Neoderm-E versus excised human cadaver skin, (e): LabCyte EPI-model versus excised human cadaver skin, and (f): Episkin versus excised human cadaver skin. Each point represents the mean ± S.E. (n=4-6).

2.32 (r = 0.8162) (no significant correlation), log P_{human} = 0.937 × log $P_{LabCyte\ EPI\text{-}model}$ - 0.759 (r = 0.3894) (no significant correlation) or log P_{human}= 0.768 × log $P_{Episkin}$ - 1.17 (r = 0.8162) (no significant correlation), respectively. These cultured skins did not show good correlations with log *P* values in excised human cadaver skin. (Figures 3 and 4)

2. Comparison of KL and DL^{-2} between each cultured skin model and excised human cadaver skin

Figure 5 shows double logarithm plots of *KL* and *Ko/w* of chemical compounds. Although the log *KL* of ANP in LSE-high was slightly higher than that in excised human skin, the other log *KL* in LSE-high was almost equal to that in excised human skin as shown in Fig. 5a. A similar set of results were obtained in our previous study (Watanabe *et al.*, 2001). The log *KL* values in EpiDerm increased by an increase in log *Ko/w* of the chemical compound as shown in excised human skin. All of the log *KL* values in EpiDerm, however, were lower than those in excised human cadaver skin and the differences were especially marked by an increase in lipophilicity of chemical compounds (Fig. 5b). In Neoderm-E, Vitrolife-skin, LabCyte EPI-model and Episkin, the increment behaviors of log *KL* were not the same as those in excised human skin. Figure 6 shows double logarithmic plots of DL^{-2} and *Ko/w* between each cultured human skin model and excised human skin. Although the log DL^{-2} in cultured human skin models was higher than in excised human skin, the log DL^{-2} values over the present log *Ko/w* values were almost constant, as shown in excised human skin. (Figures 5 and 6)

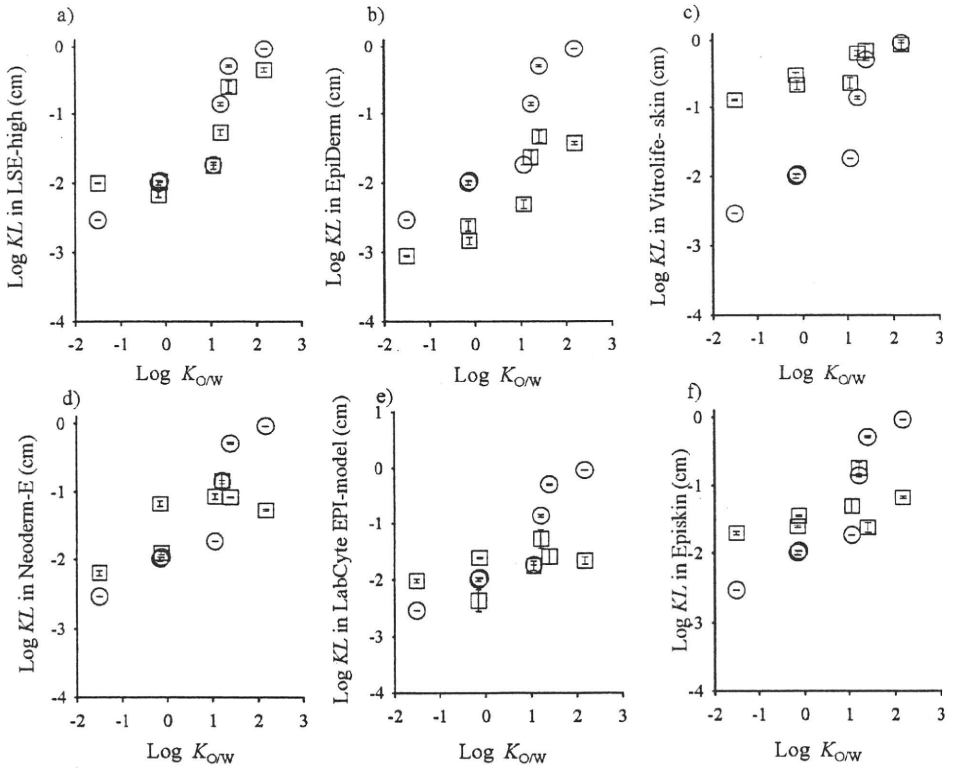

Figure 5 Relationships between log *KL* values in cultured skin models and log *K*o/w values of chemical compounds. (a): LSE-high, (b): EpiDerm, (c): Vitrolife-skin, (d): Neoderm-E, (e): LabCyte EPI-model and (f): Episkin. Symbols: ○; human skin, □; cultured skin model. Each point represents the mean ± S.E. (n=4-6).

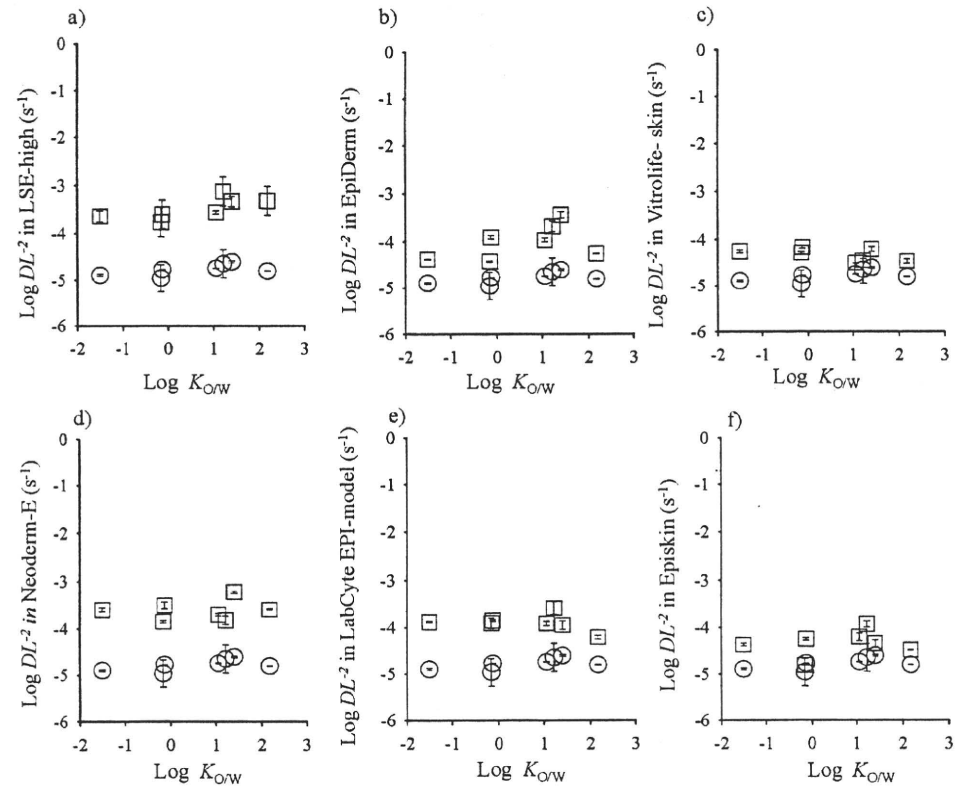

Figure 6 Relationships between log DL^{-2} values in cultured skin models and log *K*o/w values of chemical compounds. (a): LSE-high, (b): EpiDerm, (c): Vitrolife-skin, (d): Neoderm-E, (e): LabCyte EPI-model and (f): Episkin. Symbols: ○; human skin, □; cultured skin model. Each point represents the mean ± S.E. (n=4-6).

Discussion

P values of chemical compounds in cultured skin models except for EpiDerm were much higher than that through excised human skin. Other reports also revealed that cultured skin models showed higher *P* values of chemical compounds because of a low barrier function (Netzlaff *et al.*, 2007). Evaluation of cultured skin models as skin permeation models is mainly focused on the comparison of permeation curves and/or *P* values of chemical compounds between the cultured skin model and excised human skin. A 1:1 relationship in *P* values between human skin and cultured skin model would be best to predict *P* values in excised human skin from that of a cultured skin model. Thus, evaluation of the correlation slope of *P* values would be necessary to use a cultured skin model as an alternative membrane for skin permeation experiments. When the correlation slope in log *P* values between excised human skin and a cultured skin model is larger or smaller than slope 1.0 (1:1 relationship), a slight difference in *P* value through a cultured skin model would lead to a much larger difference in the estimated *P* value through human skin. Therefore, this type cultured skin model would be unattractive as an alternative membrane for skin permeation experiments.

We (Watanabe *et al.*, 2002, Kano and Sugibayashi, 2006, Sugibayashi *et al.*,2002) have already reported that the extent of skin irritation by chemical compounds was related to their concentration in viable skin tissues. Thus, a good correlation was observed between skin irritation (MTT assay result) and chemical compound concentration in the skin. We also reported recently that skin concentration of chemical compounds can be determined by the *KL* and *P* determined by obtained values from skin permeation experiments (Sugibayashi *et al.*, 2010).

The log *KL* increased with an increase in the lipophilicity of the chemical compound applied. The obtained log *KL* values in cultured skin models, however, were different to those in excised human cadaver skin, except for LSE-high. When a chemical compound is applied, it rapidly distributes into skin. The extent of distribution of the chemical compound into skin depends on its partition coefficient into skin. The outmost layer of skin, the stratum corneum, is a highly lipophilic membrane. The structure of the stratum corneum is thought to be like "bricks and mortar" (Williams *et al.*, 1987): the corneocytes and intracellar lipids are the bricks and mortar, respectively. Therefore, the composition in lipids (extracellular layer of corneocytes) and lipid structure may be important determinants of the partition coefficient of chemical compounds from the applied vehicle into skin. A comparison of total extracellular lipid compositions among cultured skin models such as EpiDerm and Episkin and human skin were reported by Ponec *et al.* (2000). They mentioned that the lipid compositions in cultured skin were different to those in human skin. The constitution ratio of total lipids in a cultured skin model is necessary to understand the features and extent of lipophilicity of the stratum corneum barrier. The reason for the *KL* differences among cultured skin models has not yet been fully explained. Further investigation will be needed to clarify the differences.

The DL^{-2} in both a cultured skin model and excised human cadaver skin were almost constant independent of the *Ko/w* of applied chemical compounds. Every cultured skin model has ahigher DL^{-2} than excised human cadaver skin. The intrinsic diffusion coefficient (*Dt*) in solvent can be obtained by the Stokes-Einstein equation and is a function only of the molecular weight. The *D* in DL^{-2} represents the apparent diffusion coefficient (*Da*) (Young and Ball, 1998; Desai *et al.*, 1965) and the *Da* composed of toutosity, effective permeation area and truth diffusion coefficient. Intracellular (stratum corneum; brick) and extracellular (intracellular spaces in the stratum corneum; mortar) pathways are well known as the diffusion route in skin permeation for chemical compounds and the predominant permeation route of chemical compounds is an extracellular route (Naik *et al.*, 2000). Thus, a different DL^{-2} suggests differences in permeation pathways in cultured human skin.

Although total intracellular lipid constitution and X-ray small angle scattering analysis (Ponec *et al.*, 2000; Hatta *et al.*,2001) were not performed to evaluate cultured skin models in the present study, the results suggested that the